ＩＳＳＮ１３４６－７８４０

港湾空港技術研究所資料

TECHNICAL NOTE

OF

THE PORT AND AIRPORT RESEARCH INSTITUTE

No.1353　August 2019

遠心模型実験装置 PARI Mark II-R の開発

高橋　英紀
藤井　愛彦
森川　嘉之
高野　大樹

国立研究開発法人　海上・港湾・航空技術研究所

National Institute of Maritime,
Port and Aviation Technology, Japan

CONTENTS

遠心模型実験装置 PARI Mark II-R の開発

高橋　英紀*・藤井　愛彦・森川　嘉之***・高野　大樹*****

要　旨

遠心模型実験装置は，土木構造物の模型に遠心力を加え，地盤内の応力や間隙水圧を高めて，実物スケールの構造物と同様の応力・間隙水圧状態を再現するものである．現在では，地盤工学分野において，実物スケールの構造物での地盤挙動を知るための重要な装置となっている．対象も静的問題，動的問題，流体と地盤の複合問題などに検討対象が拡がってきている．一方，沿岸域や海域においては，巨大地震や津波，高潮・高波に対する土木構造物の安定性を確保するため，その挙動を解明することが急務となっている．この流れを受けて，当研究所において 20 年以上使用してきた遠心装置 2 号機を改修し，巨大地震を再現したり，波や流れを発生したりできる装置を導入することとした．なお，上記の新たな実験ニーズへの対応に加えて，老朽化部分の更新も目的とした．作業は 2016～2018 年の間の 2 カ年で行った．本稿では，更新した機器や新設の装置を中心的に紹介している．なお，2 号機改良型の全体像を把握できるように，遠心装置 1 号機と 2 号機の導入経緯や，2 号機から 2 号機改良型に流用している部品についても概説する．

キーワード：遠心模型実験装置，振動台，造波装置，越流装置，画像解析

* 地盤研究領域地盤改良研究グループ長
** 国土交通省四国地方整備局（前・地盤研究領域地盤改良研究グループ　研究員）
*** 地盤研究領域長
**** 地盤研究領域地盤改良研究グループ　主任研究官
〒239-0826　横須賀市長瀬3-1-1　港湾空港技術研究所
電話：046-844-5055　Fax：046-844-0618　　e-mail:takahashi-h@p.mpat.go.jp

Development of Hydro-Geotechnical Centrifuge PARI Mark II-R

Hidenori TAKAHASHI*
Naruhiko FUJII**
Yoshiyuki MORIKAWA***
Daiki TAKANO****

Synopsis

A centrifuge machine increases stress and water pressure in a model ground with a centrifugal acceleration and produces the same behaviours as that in a prototype-scale structure. This machine is one of the most frequently used experiment tools in the geotechnical engineering field for examining the movement of prototype-scale structures. The research themes range from static problems to seismic ones, including earthquake and ocean waves. In ocean and coastal areas, there are needs to elucidate ground behaviours under a large earthquake, tsunami, and high tide and waves for ensuring the stability of civil engineering structures. Therefore, our research institute decided to introduce new systems and equipment which can reproduce large earthquakes and generate waves and flows in a centrifuge by renovating the second machine owned by our institute for more than 20 years. A secondary purpose of the renovation is to update old parts used for a long time. The renovation work was carried out over two years between 2016 and 2018. This paper introduces updated and newly installed devices, and it also includes the history of our centrifuge machines and some parts that were reused from the second machine to aid the readers to easily understand the machine in its entirety.

Key Words: centrifuge machine, shaking table, wave generator, water supply tank, image analysis

* Head, Soil Stabilization Group, Geotechnical Engineering Division
** Ministry of Land, Infrastructure, Transport, and Tourism (Formerly, Port and Airport Research Institute)
*** Director, Geotechnical Engineering Division
**** Senior Researcher, Soil Stabilization Group, Geotechnical Engineering Division
3-1-1 Nagase, Yokosuka, 239-0826 Japan
Phone：+81-46-844-5055 Fax：+81-46-844-0618 e-mail:takahashi-h@p.mpat.go.jp

1. Introduction

A centrifuge machine increases stress and water pressure in a model ground by adopting a centrifugal force; it can produce the same conditions in stress and water pressure as those in a prototype-scale structure. Figure 1.1 shows the conceptual diagram. As most behaviours of ground deformation and failure are dependent on stress and water pressure, a centrifuge model test can simulate the movement of prototype-scale structures. Meanwhile, not all behaviours of the ground movement can be reproduced because some similitude laws are not satisfied only by increasing stress and water pressure; other issues such as effects of soil particle size and the Coriolis force also need to be considered. A centrifuge modelling is not versatile; therefore, it needs skills to model prototype-scale structures and interpret test results appropriately. The adequate management of a centrifuge model test will bring success on comprehending the mechanism of ground behaviours.

Historically, Edouard Phillips, a French engineer, proposed the idea of a centrifuge modelling technique in 1869 (Phillips, 1869a; 1869b). After about 60 years, Bucky in USA and Pokrovsky & Davidenkow in USSR produced the first machines simultaneously in 1931 (Craig, 2002). After the second world war, full-scale centrifuge machines were developed at Cambridge University in UK and Osaka City University in Japan simultaneously in 1969 (Avgherinos & Schofield, 1969; Mikasa et al., 1969). Since then, many universities and institutes introduced their own centrifuge machines, including our research institute, PARI (formerly PHRI). In 1980, the institute produced the first machine, which was the largest centrifuge in Japan (Terashi, 1985).

The research themes in 1960s and 1970s were about static problems such as slope stability, bearing capacity, and earth pressure. Some researchers were sceptical about centrifuge model tests at that time, and therefore, several basic tests were conducted to show the efficacy of centrifuge modelling and to establish methods for producing model grounds. In the 1980s, the research theme expanded to consider seismic problems such as earthquakes by developing a shaking table which could work in the centrifuge. Our research institute also developed its first shaking table in 1987 (Kazama et al., 1988; Inatomi et al., 1988). Model tests on liquefaction were also carried out using the shaking table and the method of viscous scaling. Several institutes adopted a laminar shear box which could be used in the centrifuge.

The efficacy of a centrifuge model test has been known at present, and it becomes one of the most frequently used experiment tools in the geotechnical engineering field. After 1990, the number of centrifuge machines increased globally, and there are more than 100 at least. Geotechnical problems in ocean and coastal area were also recently added to the research theme of the centrifuge. Sekiguchi & Phillips (1991) developed a wave generator and conducted centrifuge model tests regarding liquefaction due to wave cyclic loading. After that study, centrifuge model tests to examine the ground behaviour subjected to ocean waves were not proactively conducted compared to those for seismic earthquake problems. However, it has recently become more important to understand ground behaviours subjected to waves in oceans and coastal engineering owing to topics such as ocean development in the open sea, construction of wind turbines, natural disasters such as typhoons and tsunamis, submarine landslides, and sea level rise. Our research institute also developed its first wave generator in 2009 (Takahashi et al., 2010) and investigated the stability of the sea shore.

Fifty years have already passed since full-scale centrifuge machines were developed in UK and Japan, and it has now become an indispensable device in the geotechnical engineering field for simulating ground behaviours. The research theme expanded from static problems to seismic ones including earthquakes and ocean waves. In our research areas (ocean and coastal ones), there is a need to elucidate ground behaviours under a large earthquake, tsunami, and high tides and waves for ensuring the stability of civil engineering structures. Therefore, our research institute decided to introduce new systems and equipment which can reproduce large earthquakes and generate waves and flows in the centrifuge by renovating the previous

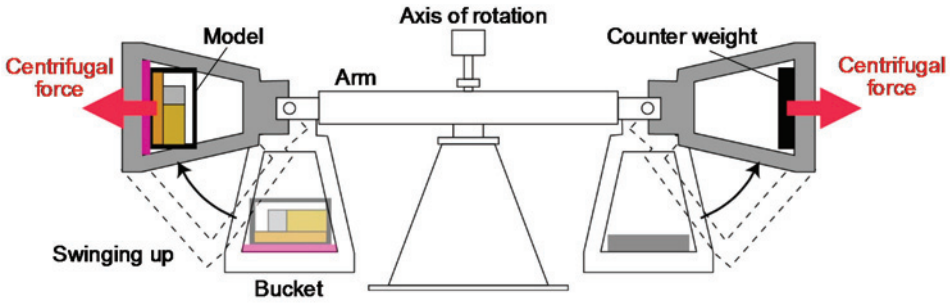

Figure 1.1 Conceptual diagram of centrifuge model test

machine owned by our institute. The renovation work was carried out over two years between 2016 and 2018. The primary purpose of this renovation was to introduce new systems and equipment to address new experimental needs as described above. In addition, we updated old parts so that we can use the machine for many years in the future; this was the secondary purpose. This paper introduces primarily the updated and newly installed devices, but it also includes the history of our centrifuge machines and some parts that diverted from the second machine for readers to easily understand the machine in its entirety.

2. Overview of PARI Centrifuge

2.1 History and specification of centrifuge

(1) First machine – PHRI Mark I

Our research institute developed the first machine, named Geotechnical Centrifuge PHRI Mark I, in 1980 (Terashi, 1985). Figure 2.1 (a) shows the machine; it was a beam-type one, and the effective radius, maximum payload, and maximum centrifugal acceleration were 3.8 m, 2710 kg, and 115*g*, respectively. Peripheral facilities such as a motor and reduction gears were located on the ground floor. The main arm and buckets were arranged on the first basement (B1F). A centrifugal force swung buckets up, and they were seated at back plates attached to edges of the main arms. The unification of arms and buckets could downsize buckets and axle bearing. Moreover, the mass of a rotating body became large and could reduce malefic vibration caused by an experiment. This method referred to the centrifuge machine designed by Cambridge University (Avgherinos & Schofield, 1969).

The construction of the first machine started in 1977 and it took three years for completion. As no manufacturer was experienced in manufacturing a large centrifuge at that time, there were several problems with selecting a manufacturer, planning, and design. Even after the completion of the machine, operations not related to research, for example adjustment of the machine and *g*-proof tests for attachments, accounted for about half of the total operations. The efforts invested during this period improved the techniques largely for a centrifuge model test, and it led to successful operations later.

The model tests using the first machine were for geotechnical problems such as measuring the bearing capacity of the ground and the horizontal resistance against a pile. Ground reinforcement and improvement methods were also developed by many centrifuge model tests, including geotextile, sand compaction pile, and cement deep mixing. In addition, the machine took an important role for solving problems which occurred at real construction sites. The operation records of the first machine were summarised in the report by Kitazume & Terashi (1994).

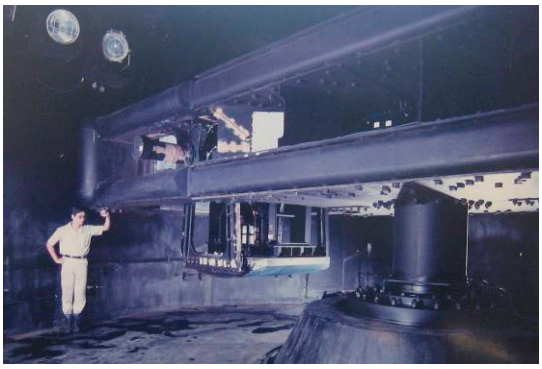

(a) First machine PHRI Mark I

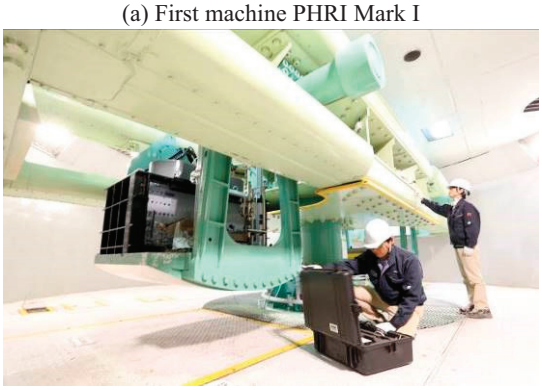

(b) Second machine PHRI Mark II (PARI Mark II)

(c) Renovated second machine PARI Mark II-R

Figure 2.1 Centrifuge machines of PHRI and PARI

(2) Second machine – PHRI Mark II (PARI Mark II)

After a few years, the first machine experienced damaging vibrations due to a structural problem. The upper floor, upper axle-bearing, and gear box vibrated during high-speed rotation owing to the thermal expansion of the central axis, and the expansion induced some cracks in the upper floor. Experiments at high-speed rotation were limited to ensure safety. Since a considerable amount of time and budget were required to solve the defects, a second machine was developed instead of repairing the first one.

The second machine was designed to solve the

problems of the first machine and to conduct model tests conveniently (Kitazume & Miyajima, 1995). Figure 2.1 (b) shows the second machine, named Geotechnical Centrifuge PHRI (PARI) Mark II. It took five years to conduct surveys and design the machine, and the construction was completed in 1994. This machine had peripheral facilities such as a motor, reduction gear box, and oil hydraulic system unit in the basement under the pit. This could improve workability for experimenters and decrease undesired noise. The size and effective radius were almost the same as the first machine because the main arm was reused for the second machine. The vibration problem of the first machine was solved by changing the structure of the upper axle-bearing. There were many means to improve workability: for example, devices such as electric powered gates at a carrying in/out port and air conditioners in the pit were introduced in the second machine. The air conditioners reduced humidity in the basements which caused rust. In addition to this, the colour of the machine and walls was changed from black to light colours, which helped elevate the feeling of experimenters. After the completion of the machine, many adjustments were required to account for the seating devices of buckets and peripheral facilities. It took five years of design and construction to get the machine to operate at its full capacity.

The model tests using the second machine were conducted on many themes: ground improvement for clayey soils such as the sand compaction pile and deep mixing methods (Takahashi, 2008; Kitazume & Maruyama, 2006; 2007), horizontal resistance against a pile and sheet piles (Kikuchi et al., 2001; Kitazume et al., 2003), active earth pressure of treated soil (Kitazume et al., 2003), liquefaction countermeasure by cement treatment and compaction grouting methods (Takahashi et al., 2013; 2016; Nishimura et al., 2011; Takano et al., 2013), ground improvement using the jet grouting method (Morikawa et al., 2014), and stability of breakwaters under tsunami (Takahashi et al., 2014; 2015). Other model tests were also conducted to solve problems in real construction sites. The second machine made a substantial contribution to research, design, and execution. Their details can be seen in each report.

(3) Renovated second machine – PARI Mark II-R

Several natural disasters such as a large earthquake, tsunami, and high tides and waves occurred in Japan, including the Great East-Japan Earthquake in 2011. It is important to secure the stability of civil engineering structures against recurring natural disasters. Therefore, it was decided that the second centrifuge machine be renovated, and special devices were installed in the machine to simulate large earthquakes, tsunamis, and waves. Some devices such as a motor and shaking table deteriorated because of operating the machine for more than 20 years. The unexpected defects might hinder continuous experiments, and therefore, it was decided to renovate the second machine. The system of the second machine was highly sophisticated, and there was no need to redesign a machine from the start. In addition, the machine should make effective use of the underground pit, experiment building, non-rusted iron components, and recently renewed equipment. This was why the second machine was reused for the successor.

Figure 2.1(c) shows the renovated second machine, named Hydro-Geotechnical Centrifuge PARI Mark II-R. It took two years between 2016 and 2018 to design and update this machine. When the second machine was developed, there were many engineers and researchers who were engaged in the development of the first machine. They had previous experience and knowledge for designing a centrifuge owing to the construction of the first machine. However, they had already retired from the company and institute, and we had to challenge renovation with low knowledge at this time. The design/construction documents were useful, and listening to people engaged in the development of the second machine was beneficial. It should be noted that it is important to transfer technology appropriately.

Figure 2.2 shows the schematic of the renovated second machine, and Table 2.1 summarizes the specifications. The electrical power equipment and upper axle-bearing were located on the ground floor. The pit containing main arms, buckets for tested models, and lower axle-bearing sustaining the central axis were on the first basement (B1F), and the motors, reduction gear box, and hydraulic power unit were on the second basement (B2F). The lubrication system and lower rotation axis were installed on the third basement (B3F). The effective radius, maximum payload, and maximum centrifugal acceleration were 3.8 m, 2760 kg, and 113*g*, respectively, corresponding to those of the second machine. The updated devices were cowls, buckets, air-intake equipment, motors and their controllers, reduction gear box, shaking table, hydraulic power unit for the shaking table, and coating. The newly installed device was a wave and current generator. The details of each equipment are listed in the following chapters.

2.2 Operation record

Figure 2.3 shows the numbers and total hours of operation from 1980 when the first machine was used. Figure 2.3 distinguishes the purpose of the operation into research and others (non-research work), as far as the records are available. The average number of operations of the first machine was 93 times per year; that of the second machine was 73 times per year. One of the reasons that the second machine was operated for a less times than the first one was because of the decrease in operations not directly related to research, such as maintenance, as

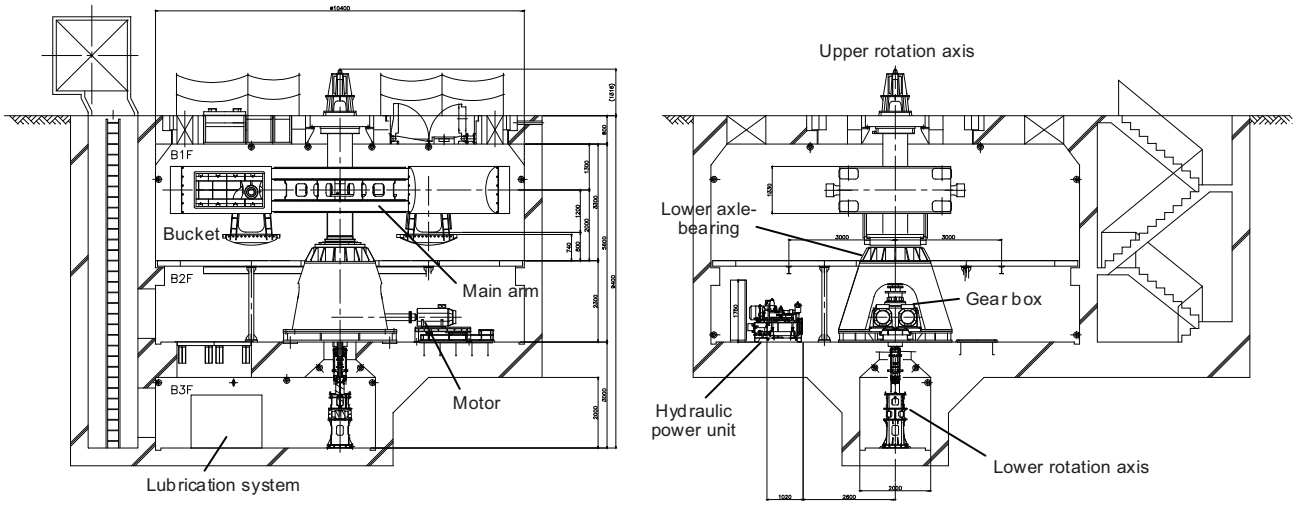

Figure 2.2 Layout of PARI Mark II-R

Table 2.1 Specifications of PARI Mark II-R

Maximum centrifugal acceleration		113*g*
Maximum payload		2,760kg
Diameter of rotating arm		9.65m
Effective radius (at platform)		3.8m
Maximum number of rotation		163rpm
Main motor	Rated output	200kW×2
	Voltage	AC440V
	Rotational speed	1,500rpm
Reduction gear	Reduction ratio	1:10
	Lubricating system	Forced lubrication
Platform	Size (Model side)	1,700×1,600mm
	Size (Weight side)	1,600×1,600mm
Rotary joint (Oil pressure)	Maximum pressure	35MPa
	Maximum flow rate	65ℓ/min
	Number of port	3
	Amount of leak	2ℓ/min×2port

Rotary joint (Water pressure)	Maximum pressure	1000kPa
	Maximum flow rate	120ℓ/min
	Number of port	2
Rotary joint (Air pressure)	Maximum pressure	1000kPa
	Maximum flow rate	120ℓ/min
	Number of port	1
Slip ring (Electric power)	Number of electrode	4
	Allowable current	30A (AC200V)
Slip ring (Control)	Number of electrode	44
	Allowable current	1A (AC100V)
Optical slip ring	Capability	1Gbps
	Number of channel	1
Lubrication system	Pressure	600kPa
	Discharge	63ℓ/min
Hydraulic power unit	Maximum pressure	35MPa
	Discharge	60ℓ/min

shown in Figure 2.3. The second machine was operated in a stable manner with a small number of maintenance operations, and it was an environment for researchers to concentrate on research. In the period when the second machine began to be used, the research theme expanded from sandy ground to a clayey one. A model test using clay takes a longer time for preparing a model, and it also reduces the number of test cases. This is another reason why the number of operations decreased in the second machine. For 38 years since 1980, when the first machine was developed, there were no severe failures that would make it impossible to operate the machine, and it could be said that it is a superior machine capable of stable operations.

The research theme of our centrifuge machines expanded from static problems to seismic problems and problems on the ground behaviours subjected to waves. In the period of the first machine, most tests were about static problems such as bearing capacity and horizontal resistance; thereafter, several seismic tests reproducing an earthquake were carried out using the second machine. The number of tests using waves has recently increased. In the future, the proportion of the test purpose is expected to change according to research needs. The centrifuge itself can be used to respond to those needs, and it can be said that the machine is a standard platform in the geotechnical field.

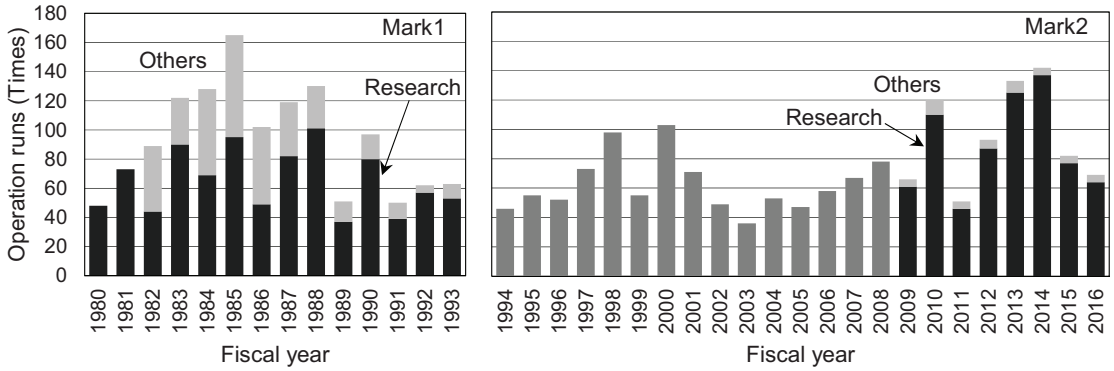

(a) Number of test

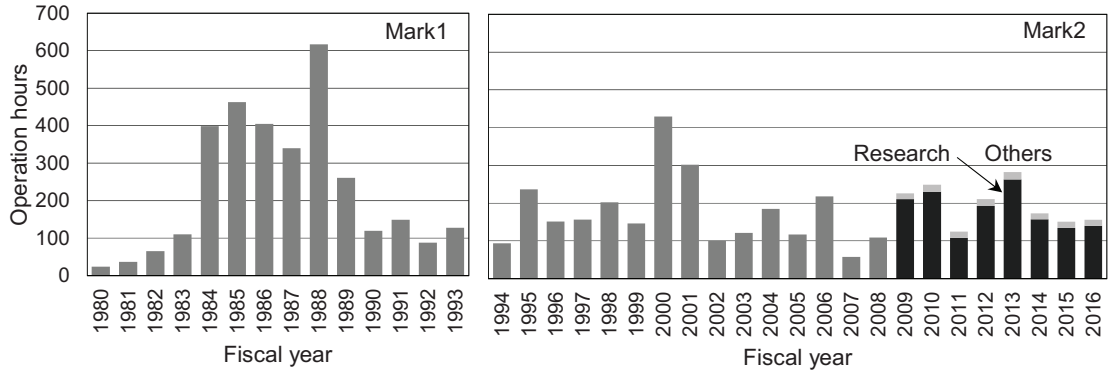

(b) Total time of rotation

Figure 2.3 Operational record of PHRI and PARI centrifuges

3. Main Unit of Centrifuge

3.1 Main frame and buckets

(1) Renewal of cowls

The central axis, main arms made of four square steel pipes, and back plates at the both ends of the arms were reused in the renovated second machine. On the other hand, the cowls and buckets were renewed. As described later, it was necessary to reduce air resistance during rotation because of the reduction of motor capacity. This resulted in the large cowls to be attached to the main arms after removing the small cowls. Figures 3.1 and 3.2 show the appearance and schematic of the cowls, respectively.

In the period of the first machine and the early stages of the second machine, a tested model was photographed by a strobe camera installed outside a rotating body. The mechanism was to release the shutter at the moment the model came in front of the camera. This was why it was necessary to open the space of view between arms so that a tested model would not be hidden by a cowl. Meanwhile, cameras are installed on the platform now because a *g*-proof camera can be used and motion pictures are needed for seismic model tests. Thus, there was no problem in shielding the field of view between the arms by a large cowl.

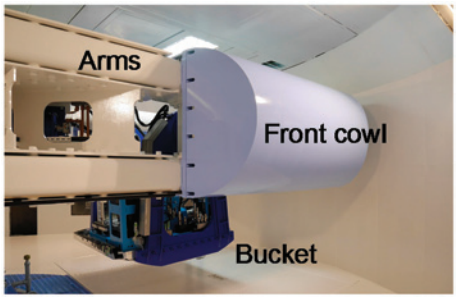

(a) Front cowl

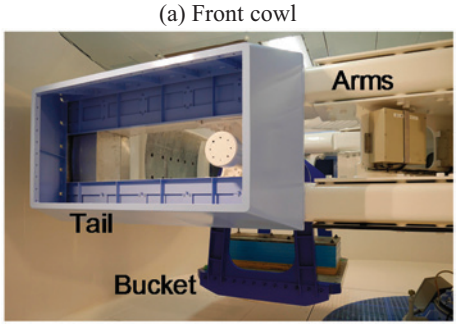

(b) Tail

Figure 3.1 Large cowl covering arms

A large cowl covering arms can reduce the wind hitting on a specimen container and air flow generated in the container during rotation. The wind in the container causes ripples on the surface of the water in the model. If the turbulence on the water surface has a harmful effect

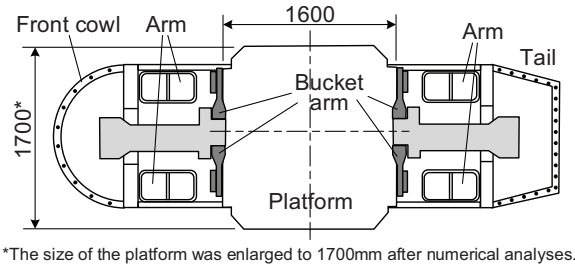

*The size of the platform was enlarged to 1700mm after numerical analyses.

Figure 3.2 Sectional view of cowl, tail, arms, and bucket

Table 3.1 Conditions and cases of fluid dynamics analyses

(a) Conditions

Reynold number	10000
Distance to front boundary	3060mm
Distance to rear boundary	6120mm
Distance to top boundary	500mm
Distance to bottom boundary	1200mm
Boundary condition (Top and bottom)	Slip
Boundary condition (Surface of object)	Non-slip
Input flow velocity	1m/s

(b) Cases

Case	Front cowl	Fairing	Tail
Org	Small (R15)	Nil	Nil
Mod1	Large (R665)	Nil	Length=665mm θ=17Deg.
Mod2	Large (R665)	Nil	Nil
Mod3	Large (R665)	Length=490mm θ=31Deg.	Length=665mm θ=17Deg.

on test results, measures such as using a cover on the top of the container were required in the previous machines. In addition, a large cowl can reduce the wind hitting on equipment such as cameras and a loading device located beside the container, and it leads to their protection.

(2) Numerical fluid dynamics analyses

The effect of large cowls was first estimated by numerical fluid dynamics analyses. The analyses were conducted by using the Reynold Average Navier-Stokes (RANS) method. This method can demonstrate time-averaged flow, averaging turbulent flow with time. The governing equations were the continuity and RANS equations. Reynolds stress can be expressed by multiplying a velocity gradient by a molecular viscosity-like variable related to turbulent stress, based on the Boussinesq's hypothesis. The software used was Open source Field Operation And Manipulation (OpenFOAM), and the calculation conditions and models are shown in Table 3.1 and Figure 3.3, respectively. The effects of a front cowl, fairing, and tail were examined in the analyses.

Figure 3.4 shows the distributions of flow velocity and pressure calculated by numerical analyses. The total drag forces are summarised in Table 3.2. The table also

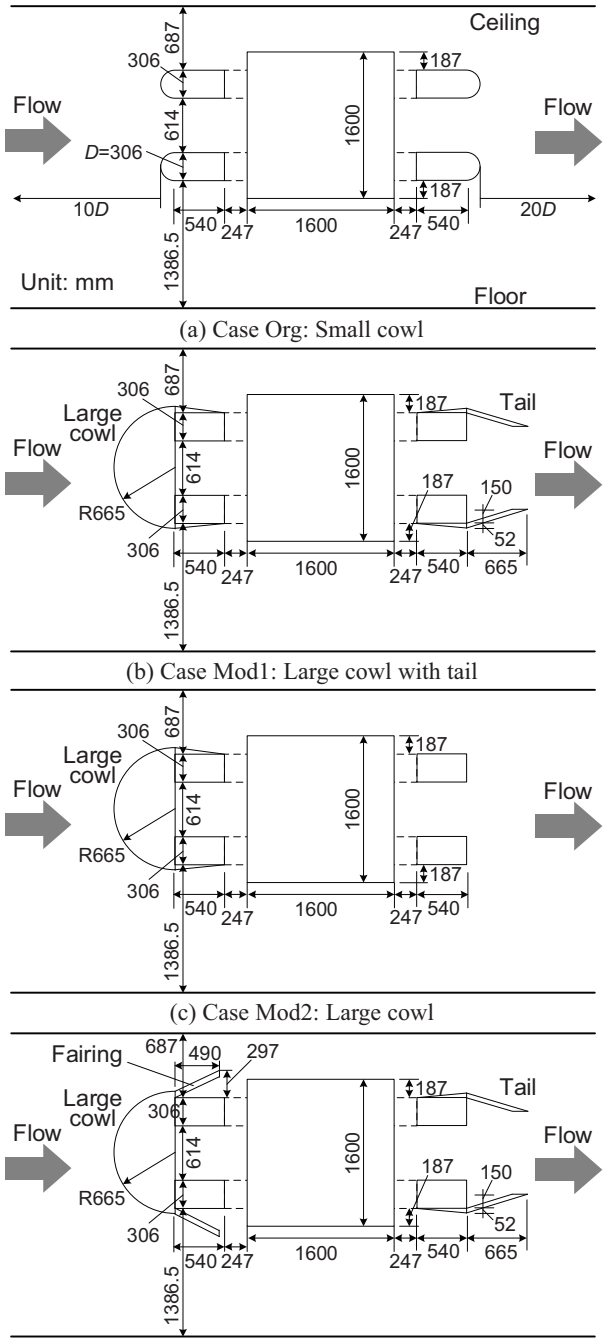

(a) Case Org: Small cowl

(b) Case Mod1: Large cowl with tail

(c) Case Mod2: Large cowl

(d) Case Mod3: Large cowl with fairing and cowl

Figure 3.3 Sectional views for fluid analyses

shows the drag forces when the input flow velocity is assumed to be 64.9 m/s at a centrifugal acceleration of 100*g*. In Case Org, without a large cowl, the wind hit on a specimen container, and the pressure increased there as shown in the figure. In contrast to Case Org, the wind flowed along the surface of a front cowl, and the pressure did not increase in other cases. As a result, the total drag force of Case Org was larger than that in other cases. For example, the drag force of Case Mod1 was 39% smaller than that of Case Org. It demonstrated the efficacy of a large cowl. Whereas, small difference among Cases Mod1,

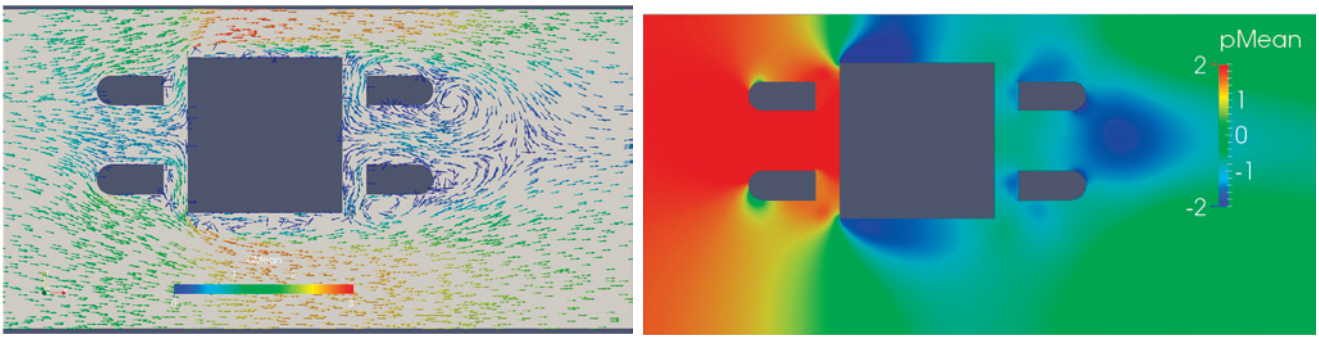

(a) Case Org: Small cowl

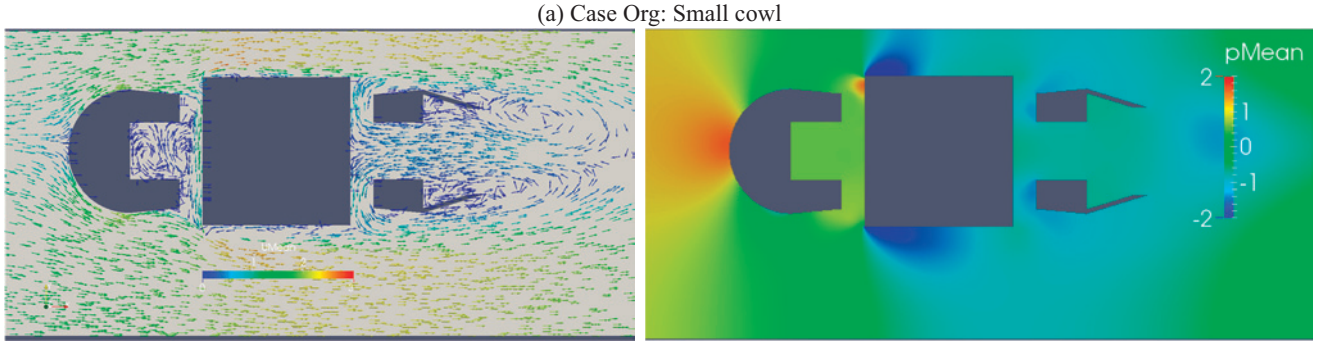

(b) Case Mod1: Large cowl with tail

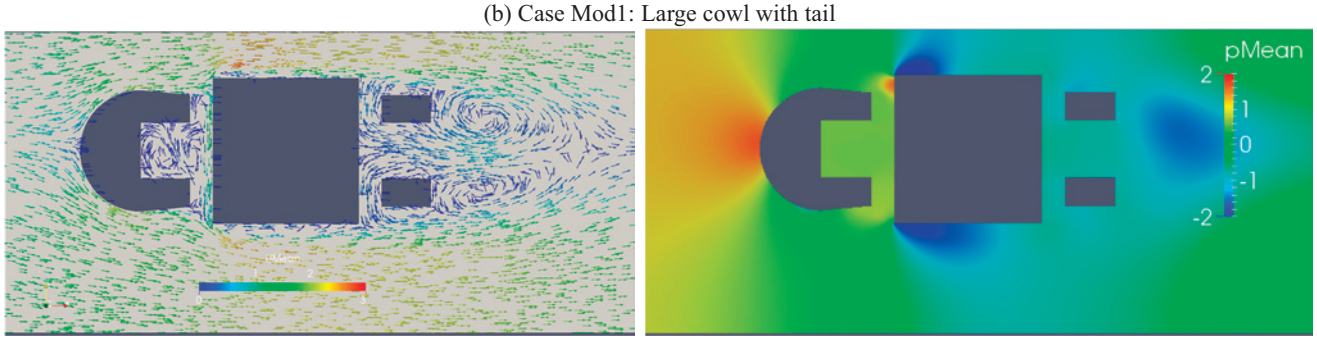

(c) Case Mod2: Large cowl

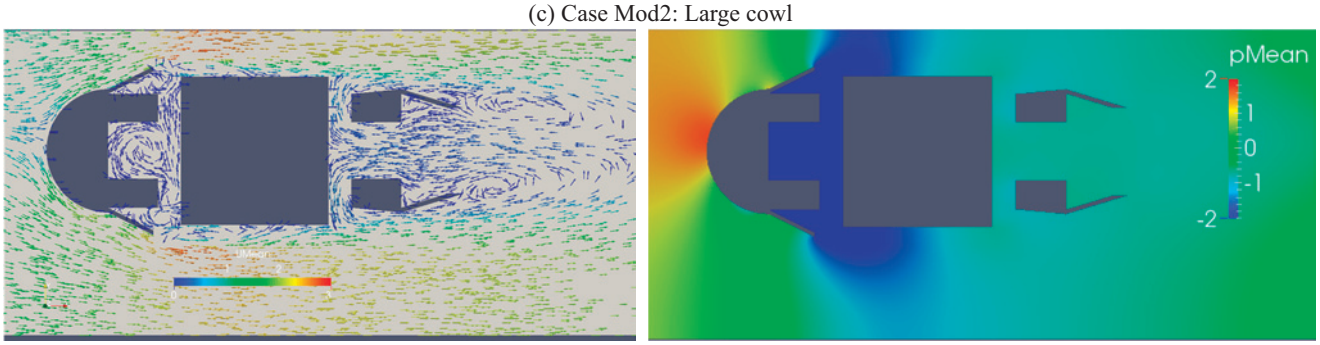

(d) Case Mod3: Large cowl with fairing and tail

Figure 3.4 Results of numerical analyses (Left: flow vector (m/s), Right: Mean pressure (Pa))

Mod2, and Mod3 indicated that a tail and fairings did not have much effect on the drag force.

(3) Prototype tests

The effect of a front cowl and fairing was also investigated using the actual centrifuge machine. As it was difficult to directly measure an air drag force, the drag forces were qualitatively evaluated by using motor torques needed for the rotation. Table 3.3 lists the test conditions. In the tests changing a cowl and fairings, the motor torque was measured when the machine accelerated at a speed of 155 rpm, corresponding to a centrifugal acceleration of 100*g*.

Table 3.2 Total drag forces acting on object

Case	Front cowl	Fairing	Tail	Force (N/m)	Force at 100*g* (N/m)
Org	Small	Nil	Nil	0.041	172.7
Mod1	Large	Nil	Mounted	0.025	105.3
Mod2	Large	Nil	Nil	0.026	109.5
Mod3	Large	Mounted	Mounted	0.027	113.7

Table 3.3 Conditions and cases of prototype tests

(a) Conditions

Centrifugal acceleration	100*g*
Number of rotation	155rpm
Angular acceleration	0.028rad/s^2
Specimen container	Mounted

(b) Cases

Case	Front cowl	Fairing	Tail
E-Org	Nil	Nil	Nil
E-Mod1	Large (R665)	Nil	Length=664mm θ=13Deg.
E-Mod3	Large (R665)	Length=362mm θ=20Deg.	Length=664mm θ=13Deg.

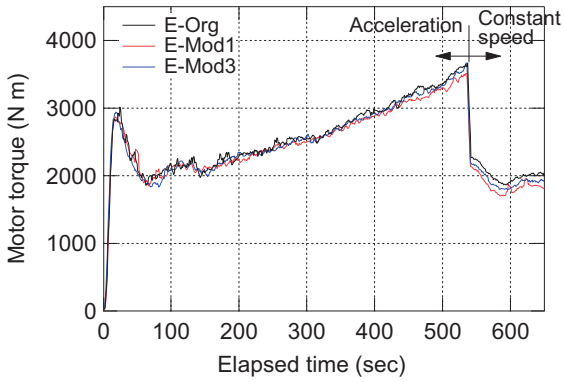

Figure 3.5 Results of prototype tests

Figure 3.5 shows the test results. The figure expresses motor torques averaged at 5 s because a motor torque fluctuates. A sudden increase in torque occurred when starting the rotation, and this would be due to the friction of the rotating system and the inertia moment of the rotating body. Next, the torque gradually increased corresponding to the acceleration of the rotation. The moment when the machine needed the largest torque was before reaching the centrifugal acceleration of 100*g*. At this point, the torque reached a peak because three torques for friction, air drag force, and inertia moment were piled up.

The peak torques of three test cases were Case E-Org: 3816 Nm, E-Mod1: 3579 Nm, and E-Mod3: 3708 Nm. Since there was no large difference in both the friction and the inertia moment in the three test cases, the differences in torque are attributed to the differences in air resistance. Smaller torques in Cases E-Mod1 and E-Mod3 demonstrated the efficacy of a front cowl. The torque in Case E-Mod1 was smaller than that in Case E-Mod3, and it indicated that the fairing attached to the main arms increased the torque. As a result, a front cowl without fairings could reduce the motor torque by 6%. The reason why fairings increased the torque can be considered as follows: the specimen container did not protrude from the edges of the arms in Case E-Mod1; in contrast, fairings protruding from the edges hindered the flow in Case E-Mod3.

The torques at steady rotation were Case E-Org: 2008 Nm, E-Mod1: 1866 Nm, and E-Mod3: 1934 Nm. The torque was small in the order of Case E-Org, E-Mod3, and E-Mod1, and 7% torque reduction was achieved with E-Mod1 for Case E-Org. This reduction also contributed to power saving, especially for a long-term operation. As a result, the installation of a cowl succeeded in reducing a significant amount of torque of 6% or 7%, although it was smaller than the reduction rate of a motor capacity of 11%. Based on these results, a front cowl was installed on the arms, but fairings were not.

The reduction rate of the total drag force calculated by numerical analyses reached 39% by installing a large front cowl and tail on the arms. On the other hand, the motor torque of the actual centrifuge machine decreased only by 6% during acceleration and 7% at steady rotation. Although the numerical analyses were carried out on the cross section, the machine is a three-dimensional rotating body. This indicates difficulty to compare the two directly, but the reason why the reduction rate in the prototype test can be expected is as follows. First, the analyses modelled the cross section at the platform which had the largest width, but most sections of the actual machine did not have this width. The angle of fairings was also narrowed to 20° in the actual machine tests. It can be said that in the prototype tests, the objects generating a drag force were small. Second, the actual machine requires motor torque against friction and inertia moment in addition to air resistance. The installation of a cowl rather tends to increase the torque.

(4) Buckets

Both buckets for a tested model and counterweights were renewed because they became old, and a larger platform for a tested model was needed. Figure 3.6 shows the renewed buckets. The platform for counterweights has a box structure made of steel plates, and that for a tested model has a solid structure made from a lump of aluminium to achieve weight reduction. The reason why it was necessary to reduce the weight of the platform was that the weight of a new shaking table was large, and therefore, the size of the platform was enlarged.

The sizes of the platform for a model are 1700 mm and 1600 mm, and the length in one direction is 100 mm larger than that of the second machine. This allows using a wider specimen container. In addition, a part on the bottom of the platform for a model was cut to reduce the weight and tilt the platform by shifting the centre of gravity. Our centrifuge machine has a structure wherein the bucket is seated on the back plate at the centrifugal

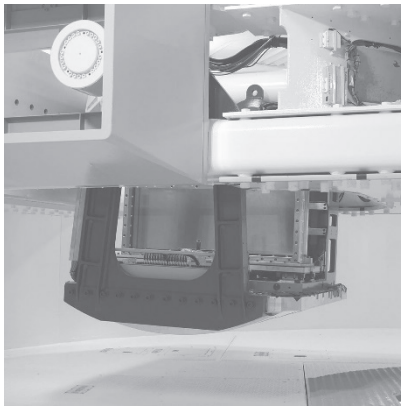

(a) Bucket for tested model

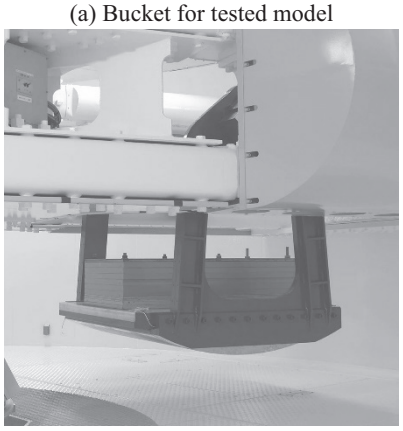

(b) Bucket for countered weights

Figure 3.6 Buckets including platforms

acceleration of approximately 20 to 30*g*. The bucket is supported by elastic springs from the rotating arms; it induced that the direction of the resultant of gravity and centrifugal forces was not perpendicular to that of the platform surface at a larger centrifugal acceleration. To solve this problem, the initial inclination angle was adjusted to approximately 2° so that the two were nearly perpendicular at the centrifugal acceleration of 50*g*, which is most frequently used.

(5) Air-intake equipment

The rotation of the main arms gradually increases temperature at the pit due to air resistance. Although a method of forcibly cooling the system with an air conditioner was adopted in the first machine, it could not suppress the temperature rise. To avoid this, an air-cooling system was adopted in the second machine, which would take in air from outside.

An air-intake equipment is located outside the building, and outside air is supplied to B2F and B3F through the duct. Air flows to the pit on B1F and the ground floor, and finally, it is discharged to the outside through a silencer on the ground floor. It flows naturally without using power. When the main arms rotate in the pit, the flow velocity increases near the ceiling and outer peripheral part, and it decreases near the floor and inner peripheral part. As a result, air flows in the direction from the centre on the floor to the outer peripheral part of the ceiling. An air inlet and outlet were installed at each position.

Figure 3.7 Air intake equipment

Since the air-intake equipment was located outdoors, corrosion proceeded and it caused an iron plate to come off. The air-intake equipment was also updated at this time. Figure 3.7 shows the appearance of this equipment. The cross section of the inlet is about 2 m × 2 m. The removal and installation of an equipment were conducted by using a large rough terrain crane.

3.2 Motor and reduction gears

The main motor of the second machine was aging, and there was a concern that it would break down and prevent continuous research work; thus, it was also updated. The motor used for the second machine was a large DC-type one of 450 kW, but an AC-type motor is recently used in the market as a large motor. This situation made it difficult to replace the motor with a same type one as it required a considerable amount of time and cost. Accordingly, it was decided that an AC-type motor will be used instead of a DC-motor. The renovated second machine adopted the system of synchronous operations of two AC motors of 200 kW because this size of motor is mass produced and is cost effective. The controllers for motors and a reduction gear box were also renewed, which corresponds to the renewal of a main motor (see Figure 3.8). Although the total capacity decreased from 450 kW to 400 kW, the decrement of 50 kW was considered to be covered by reducing the angular acceleration and air resistance with the use of cowls. After renovating the machine, it could be operated even with a motor capacity of 400 kW.

Servo motors are adopted as main motors, and these make it possible to control rotation with higher positional accuracy than before. As a regenerative braking system is used to decelerate the machine, it can save electricity.

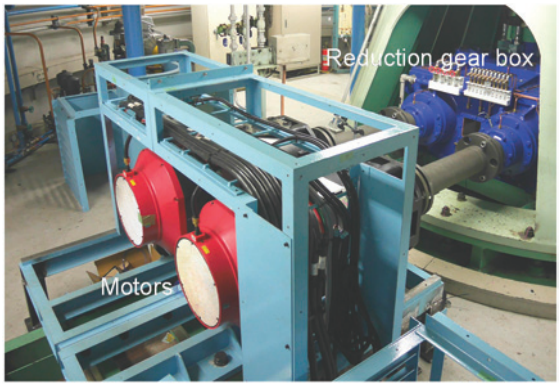

Figure 3.8 Motor and reduction gears

There is another advantage to using two motors: If one motor broke down, the other motor could still rotate the arms, although at a low speed and with a maximum acceleration of 30*g*. In the future, research work could be continued if a motor broke down, and it can be said that using two motors would reduce the risk of research suspension.

3.3 Oil hydraulic system

A shaking table and a wave and current generator (explained later) require large amounts of hydraulic power because they can move with oil hydraulic cylinders. Hydraulic power is supplied from a power unit located outside the rotating body through piping and a rotary joint. Table 2.1 lists the specifications of a power unit and rotary joint. The power unit is placed on B2F, and a rotary joint is installed to the lower rotation axis on B3F. As the new shaking table requires lager hydraulic power than the old one, a power unit was also renewed. Figure 3.9 shows a new power unit.

The new power unit can produce a high pressure of 35 MPa. Theoretical discharge is 60ℓ/min, and the capacity of a rotary joint corresponds to this discharge. The hydraulic power is also used for lubricating a rotary joint to avoid the seizure. The oil transferred from a power unit via piping and a rotary joint is supplied to the platform in the pit on B1F. Since the shaking table and the wave and current generator are detachable, it is necessary to connect them to the supply pipe for every test. A coupling-type check valve socket is adopted as a connection method to prevent oil leakage when connecting. This type of socket has a small diameter and reduces the flow rate. However, it is accepted because a new shaking table includes accumulators and a wave and current generator does not need an amount of flow rate.

There is another lubricating oil circulation system besides that for the power unit of the shaking table and the wave and current generator. This system is used for lubricating a reduction gear box and a lower axle-bearing. The oil supply tank and pump are located on B3F, and the theoretical discharge and pressure are 63ℓ/min and 600 kPa, respectively. If this oil was not supplied, for example, due to electric outage, the gears and bearings would undergo seizure. To avoid this, an emergency generator is prepared for operating the oil circulation system.


Figure 3.9 Hydraulic power unit

3.4 Air and water supply system

The machine also has rotary joints for water and air at the lower rotation axis on B3F, which can be used on the platform during rotation. For example, air pressure is used to open and close the valve quickly on the platform, and to operate an air cylinder. Water pressure can be used to move a cylinder as well as air one, and to directly supply water into a tested model. Each maximum discharge is 120ℓ/min, and the allowed maximum pressures are 500 kPa for water and 700 kPa for air, respectively. The pressure can be adjusted from a remote panel. These devices were diverted from the second machine.

3.5 Electrical power and data transfer system

Electrical power is supplied via a slip ring in the lower rotation axis on B3F, which is used to operate equipment on the platform and measuring systems in the rotating body. The capacity of the electrical power is 30 A at three-phase AC 200 V. This power is divided at a panel installed near the central axis, and it is converted to AC 100 V and DC 24 V as well. There are more than 20 wiring lines. ON/OFF signals can be sent from the control room via a relay box. This facility was also diverted from the second machine.

LAN is used for transferring data. To speed up data transfer, the wired LAN is basically used except for a part of an axle bearing, where the wireless LAN is used. As a high-speed camera requires high-capacity wires for data transfer, a 1 Gbps optical slip ring is also used at the axle bearing. There are three lines of LAN in total, each for measuring instruments at the upper axle bearing (via wireless LAN), for monitoring by cameras at the lower rotation axis (via wireless LAN), for controlling a high-speed camera, shaking table, and a wave and current generator at the upper axle bearing (via an optical slip ring). These facilities were also diverted from the second machine.

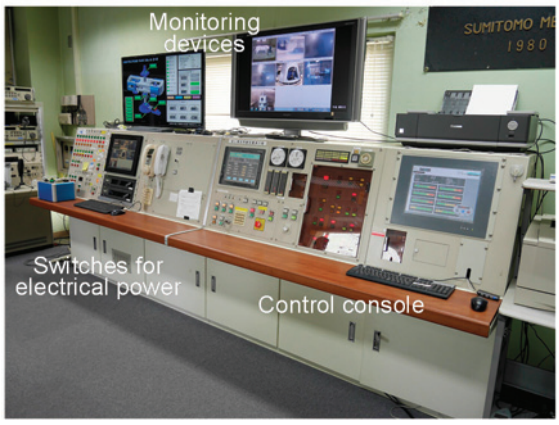

Figure 3.10 Control console board

Table 3.4 Monitoring items for safety

Instrument	Measuring object	Content
EDX	Rotational speed	Speed
	Command value of rotational speed	Speed
	Axle-bearing (at 2 points)	Vibration
	Reduction gear	Vibration
	Floor slab	Vibration
	Lubrication oil (at 3 points)	Flow rate
	Leak of rotary joint	Flow rate
	Axle-bearing (at 2 points)	Temperature
	Reduction gear	Temperature
	Drain oil	Temperature
	Motor bearing (at 4 points)	Temperature
	B1F pit	Temperature
	Lubrication system	Temperature
SPM	Axle-bearing (at 2 points)	Vibration
	Reduction gear (at 5 points)	Vibration
Discrete instrument	Oil tank in HPU (at 2 points)	Level
	Cooling water for HPU	Temperature
	Hydraulic power unit (HPU)	Temperature

3.6 Safety monitoring system

It is prohibited to enter the facility building when the machine is in operation to ensure safety. The operation of the machine, control of devices, and data measurement are conducted from a remote control room. The conditions of operation are monitored in the room by sensors and cameras attached to each equipment. Figure 3.10 shows a control panel.

The major monitoring items for safe operation are shown in Table 3.4, including accelerometers measuring the vibrations of equipment, temperature sensors for equipment and oil, and flowmeters measuring flow rates of oil. The machine is programed to decelerate automatically and start a back-up system when it detects abnormal conditions. In addition, the monitored data is constantly recorded on a computer in a control room when running the machine, and it helps reveal causes in case of emergency stops. This facility was also diverted from the second machine.

Table 3.5 Measuring instruments and channels for test

(a) Static measurement

Instrument	Number of channel
TDS-530	1ch (for measuring rotational speed)
TDS-530	9ch
IHW-50G	50ch

(b) Dynamic measurement

Instrument	Number of channel
TMR221	56ch (for 4 strain gauge)
TMR223	8ch (for 1-4 strain gauge)
TMR231	8ch (for voltage measurement)

3.7 Measuring instruments

Displacement, load, earth pressure, and water pressure need to be measured during the operation of a machine. Both static and dynamic measurements can be performed since the development of the second machine. Static measurements are used for measuring something stably at long intervals of more than 2 s; whereas dynamic measurements are measurement at short intervals of less than 2 s. As for static measurements, analogue data measured by sensors on the platform was taken out of the rotating body via slip rings on the upper rotation axis, and slip rings were connected to measuring equipment in a control room. With regard to dynamic measurements, amplifiers and A/D converters were installed in the rotating body, and the measured data was converted into digital data in the rotating body. Digital data was transferred and recorded on a computer in a control room.

As long periods passed since the development of the second machine, an amplifier and A/D converter frequently broke down. Because of that, the measurement system was updated over the period from 2007 to 2010. Table 3.5 summarises the measuring system of the renovated second machine. TDS530 and TMR200 series manufactured by Tokyo Measuring Instruments Laboratory Co., Ltd. are used for static and dynamic measurements, respectively. The numbers of the measurement points are 59 for static measurement and 72 for dynamic measurement. The measuring instruments were installed near the central axis inside the rotating body. Analogue data measured by sensors on the platform was digitised by the measuring instruments, and the data was transferred to computers in a control room via LAN.

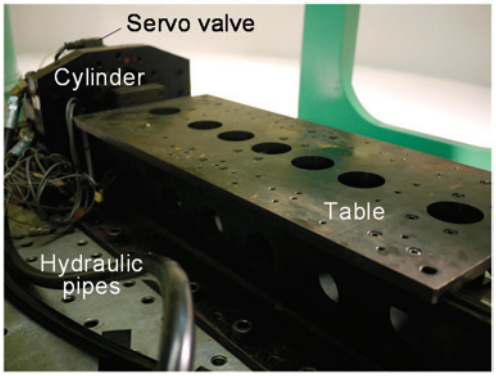

Figure 4.1 Former shaking table

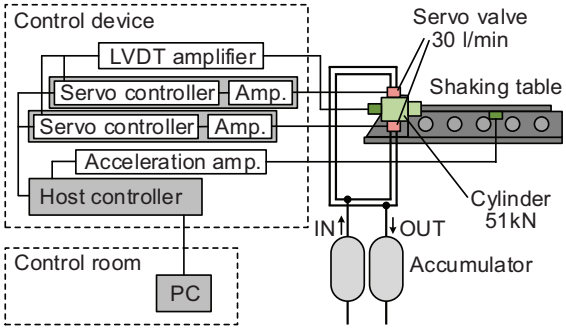

Figure 4.2 System of former shaking table

4. Mounted Apparatus

4.1 Shaking table

Our institute developed a genuine shaking table which could move with hydraulic power in 1987, and we have conducted several dynamic model tests simulating earthquakes since then. The loading capacity was 51 kN, and it was one of the most powerful shaking table at that time (Kazama et al., 1988; Inatomi et al., 1988). Around 2000, our institute started a model test regarding liquefaction by using the shaking table to investigate damages due to liquefaction and liquefaction countermeasures in port and airport facilities (Takahashi et al., 2006). Figures 4.1 and 4.2 show the appearance of the shaking table and its system, respectively. This table was detachable and installed on the platform when needed. The initial system was that the ROM in which wave data was recorded was mounted in a shaking table controller beforehand, and a computer in a control room would send a trigger for starting vibrations. This control system was updated in 2007. Wave data and a trigger could be sent from a computer in a control room in the new system. This made it possible to move the shaking table with an arbitrary waveform.

The control system was updated ten years ago, but the shaking table itself became old and had some issues. In addition, the need for experiments simulating larger earthquakes and structures increased. Therefore, the

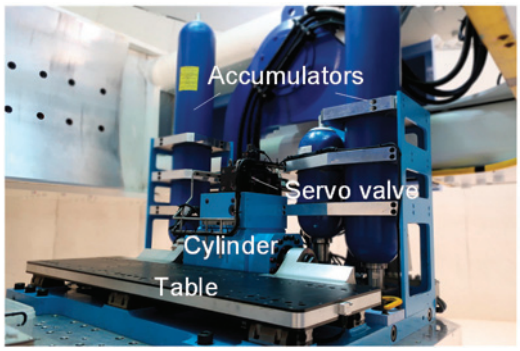

(a) Appearance

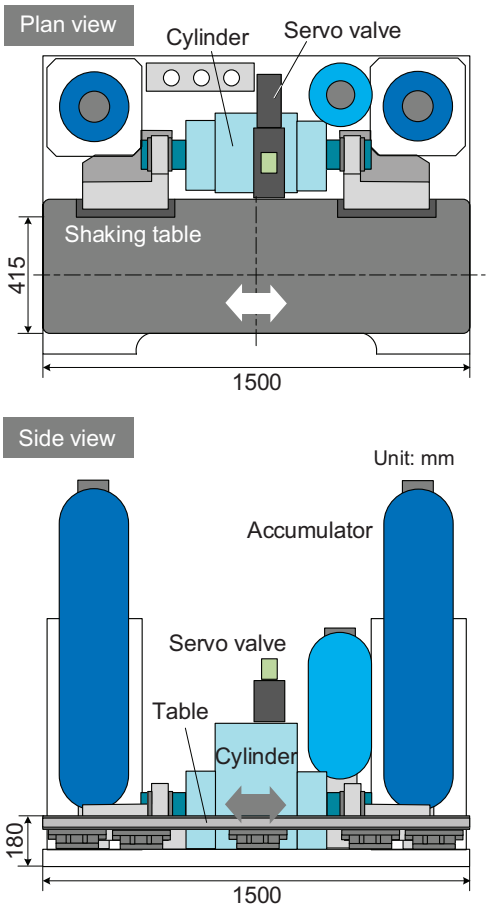

(b) Schematic drawing

Figure 4.3 New shaking table

entire shaking table was updated. Figures 4.3 and 4.4 show the appearance of the new shaking table and its system, respectively. The specifications are listed in Table 4.1. This can move with hydraulic power and is detachable like the old one. The features are listed below:

1) Maximum centrifugal acceleration and loading power

The maximum centrifugal acceleration of the old shaking table of 50*g* was raised to 100*g* for the new one. Structural members of the shaking table were designed such that they can withstand the centrifugal acceleration

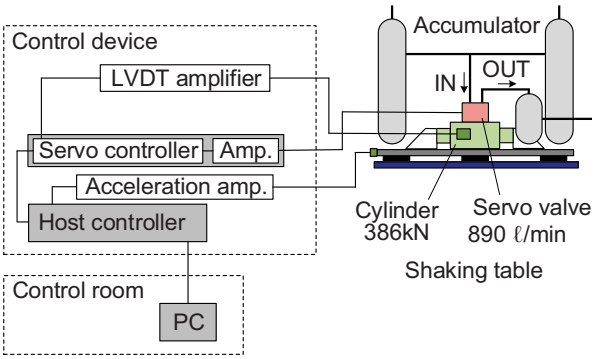

Figure 4.4 System of new shaking table

Table 4.1 Specifications of shaking table

Maximum centrifugal acceleration	100*g*
Movable frequency	10–100Hz
Maximum shaking acceleration	50*g*
Maximum shaking velocity	100kine
Movable displacement	±10mm
Maximum payload	280kg (50*g* or less) 145kg (more than 50*g*)

of 100*g*. This makes it possible to model larger structures. For example, deep-water quay walls corresponding to the enlargement of vessels are required and developed at the site, and the new shaking table enables simulating them.

Earthquake ground motion (scenario wave) expected to occur at the site is growing, and it is necessary to confirm the earthquake resistance of structures against those earthquakes. This is why the loading capacity of the shaking table has been increased. The loading capacity of the old shaking table was 51 kN, but that of the new shaking table is 386 kN. In order to increase the loading capacity, the size of the hydraulic cylinder is increased and accumulators storing hydraulic pressure are placed close to the loading cylinder. Accumulators were installed near the central axis in the old system, but in this method, energy loss occurred in the hydraulic piping during oil transporting and it was not possible to demonstrate sufficient capability.

A heavy top table was required for higher loading capacity and stronger structural members for a table itself and joint parts. In particular, a carbon fibre reinforced plastic plate was attached to an aluminium frame. The mass of the moving parts including the top table of the old shaking table was approximately 90 kg, but that of the new shaking table was approximately 60 kg. Despite spreading the table area to 156%, it can reduce the mass to 67%.

2) Table width and height

The longitudinal length of the shaking table was enlarged from 1,000 mm to 1,500 mm so that a large-size specimen container could be installed. The prototype scale increases from 50 m to 75 m in case of a model test

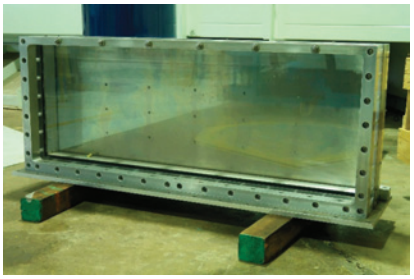

Figure 4.5 Specimen container for dynamic model test

with centrifugal acceleration of 50*g*; and it can reproduce 150 m at the centrifugal acceleration of 100*g*. As the length of the old platform was 1,600 mm and the hydraulic cylinder was placed beside the longitudinal direction of the top table, it was impossible to place a large specimen container with the inner dimension of more than 750 mm. The length of the platform was extended to 1,700 mm and the hydraulic cylinder was placed on the side of the top table, as shown in Figure 4.3. This makes it possible to place a large specimen container with the inner dimension of approximately 1350 mm. Figure 4.5 shows an example of a specimen container. In addition, the height of the top table was set to just 180 mm from the platform to make the effective radius as large as possible.

3) Hydraulic control system

The system of the old shaking table was that two servo valves synchronously controlled a hydraulic cylinder, as shown in Figure 4.2. The parallel operation of the servo valves has not recently worked well because of the aging and degradation of their balance. The shaking table, which works in the centrifuge, needs to move at a high frequency such as 50 Hz, and precise adjustment in balance and attentive maintenance are essential for parallel operation. However, it was difficult to adjust balance over a long period of time because of the considerable time and cost requirements, and it must be said that the system of the old shaking table was slightly unsuitable for us. In order to increase the loading capacity, it is easy to conceive that a servo valve and cylinder are divided for parallel operation, but the stability as a system is considered to deteriorate further.

The new shaking table adopted a simple system that is comprised of a large servo valve and cylinder. This simplicity enables to improve the stability as a system and reduce maintenance cost necessary for adjustment. However, there are two problems. First, products using large members are easily affected by a centrifugal force; second, there are no products which can move at high frequencies. As for the former problem, g-proof tests were conducted to confirm whether servo valves work in a centrifugal acceleration field before manufacturing a shaking table. Three types of servo valves (Valve 1: 890

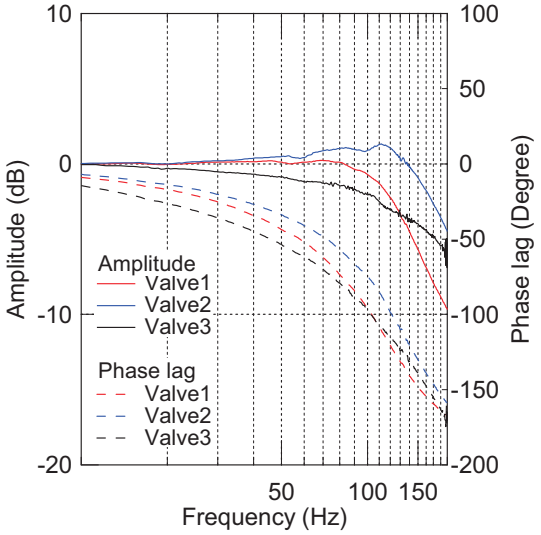

(a) Under 1*g*

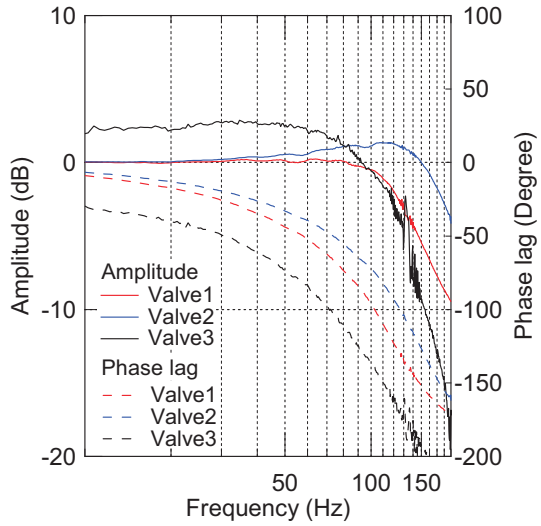

(b) Under 100*g*

Figure 4.6 Results of servo valve tests

ℓ/min made by Bosch Rexroth, Valve 2: 450 ℓ/min by Bosch Rexroth, Valve 3: 900 ℓ/min by Yuken) were tested in the centrifuge. The results are shown in Figure 4.6. As a result, all valves worked under a centrifugal acceleration of 100*g*. Of three valves, the performance characteristics of Valve 1 did not change at 1*g* and 100*g*, and the stability was the highest. In consideration of the result and other conditions, Valve 1 is adopted as a valve for a new shaking table. The second problem that there are no products that deal with high frequency. It is said that the frequency of a seismic motion which damages a port facility is about 0.5 to 2 Hz, which corresponds to 25 to 100 Hz at 50*g* and 50 to 200 Hz at 100*g*. As shown in the figure, the valve could produce vibrations up to about 100 Hz. Although there is a range that cannot be covered at 100*g*, this has to be compromised for emphasising the stability of a system.

Table 4.2 Test conditions of shaking table

Centrifugal acceleration		50*g*
Weight of specimen container		255kg
Regular wave	Waveform	Sinusoidal wave
	Frequency	50Hz
	Displacement	±1mm
Irregular wave	Waveform	Scenario wave
	Dominant frequency	50–75Hz
	Maximum acceleration	131m/s^2

As members of a servo valve are large and there is a possibility that a spool might be fixed, the new shaking table inputs a 400 Hz dither signal which is considered to have little effect on a model because of high frequency. A dither signal is a high frequency and small vibration for improving the movement of a spool in a servo valve. Moving a spool at all times can reduce a static friction force. As Tomisaka et al. (2012) pointed out that a dither signal affects vibration, this point would be a disadvantage for the new shaking table. However, it was confirmed that a 400 Hz vibration was attenuated in a test mentioned later, and its influence is considered to be not large.

4) Maximum displacement of table

The movable displacement of the old shaking table was ± 6 mm. This is equivalent to ± 0.3 m on a prototype scale when the model test is conducted under a centrifugal acceleration of 50*g*. In the Great East-Japan Earthquake in 2011, a long periodic motion became a problem, and the displacement was said to reach nearly 1 m. The displacement of ± 6 mm was unsatisfactory to simulate it; this was increased to ± 10 mm in the new shaking table, which corresponds to ± 1 m in a prototype scale under a centrifugal acceleration of 100*g*.

The features of the new shaking table are noted above, and the results of test runs are shown below. Table 4.2 summarises the test conditions. In the tests, a specimen container of 255 kg including soil materials was put on the shaking table, and it was shaken under a centrifugal acceleration of 50*g*. Figure 4.7 shows accelerations measured when the model was subjected to sinusoidal waves of 50 Hz corresponding to 1 Hz in a prototype scale. Figure 4.8 shows velocities and accelerations in a prototype scale when subjected to irregular waves. Each figure includes input signals and measured data. The results of passing through a band filter of 0.8 to 1.2 Hz for sinusoidal waves and a low pass filter of 3 Hz for irregular waves are also shown in the figures. The input and measured waveforms were similar, as shown in the figures, and they demonstrated a high performance of the new shaking table. However, the measured value tended to be larger than the input one. This phenomenon did not

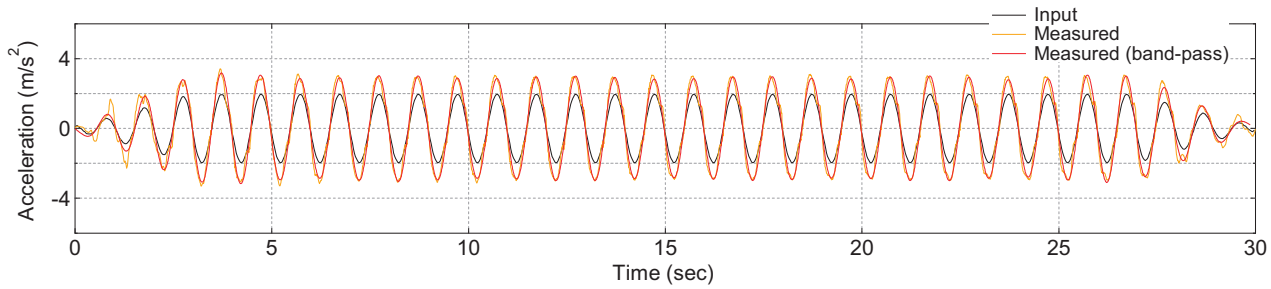

Figure 4.7 Time histories of acceleration in regular wave test (Sinusoidal wave)

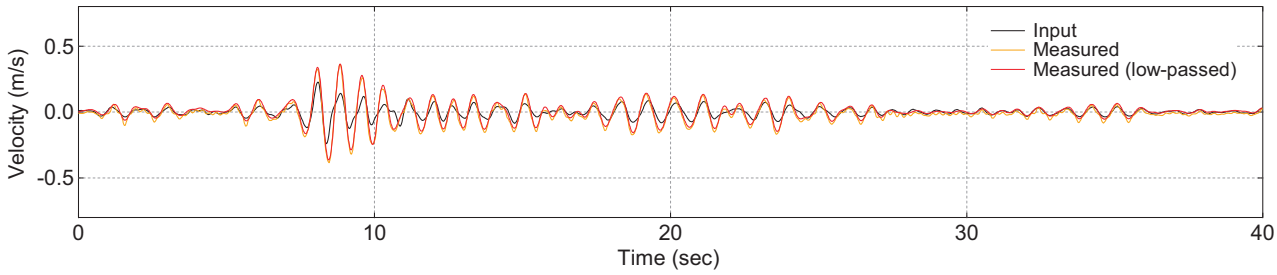

(a) Velocity

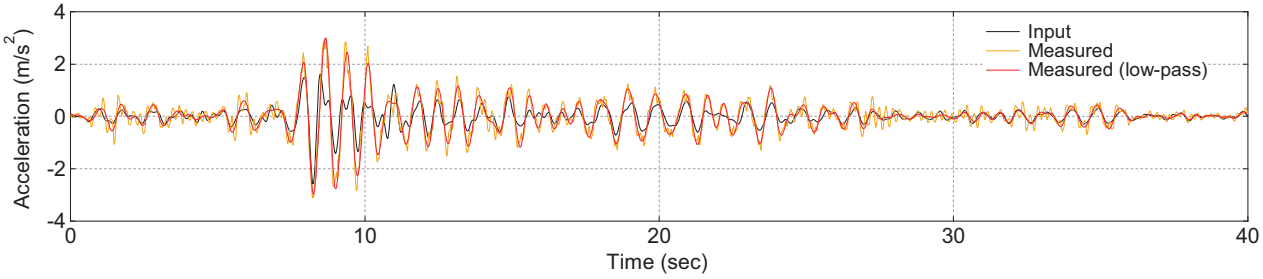

(b) Acceleration

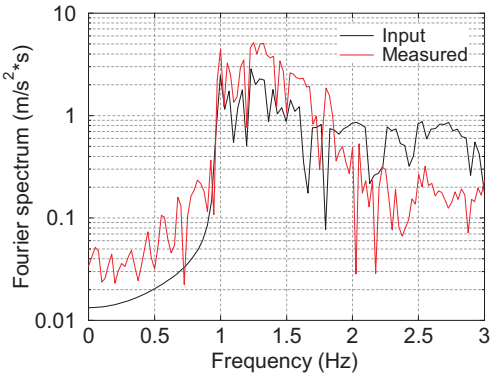

(c) Spectrum of acceleration

Figure 4.8 Result of irregular wave test

appear in a test without a specimen container. The acceleration would be amplified by the specimen container which had a large mass. It can be avoided by adjusting an input signal.

4.2 Liquefaction test techniques using shaking table

(1) Preparation of liquefiable ground

Our team has conducted several model tests simulating ground liquefaction. This section introduces techniques and equipment for a liquefaction model test. Liquefiable model grounds are usually prepared by making dry sandy ground and percolating fluid into it. This is because it enables us to produce a uniform and highly saturated ground. Dry sandy grounds can be formed by the air pluviation method wherein sand is dropped from a sand hopper (e.g., Takahashi et al., 2006). The density of the ground is adjusted by changing the size and height of the outlet of a hopper.

Our team uses two methods of fluid percolation. The

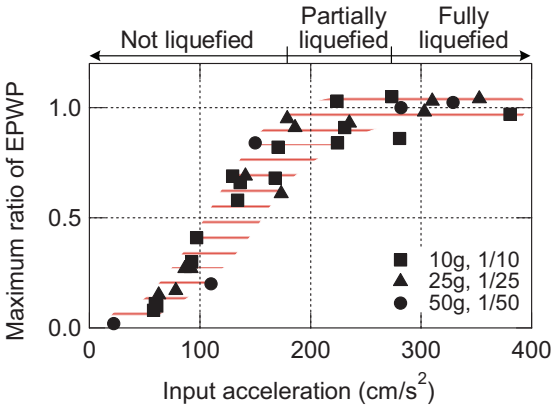

Figure 4.9 Result of modelling of models tests (based on Takahashi et al., 2006)

first one is that air in voids is replaced by CO_2 and then fluid is percolated into the ground by the water head difference under degasification. This method is usually used in an elementary test, and it has been confirmed that the ground was fully saturated (Takahashi et al., 2006). This method, however, has a disadvantage that it needs a considerable amount of time for percolation. The second method is that fluid is percolated by the water head difference in the centrifuge, which was proposed by Okamura & Inoue (2012). The period for percolation is small in this method because the centrifuge increases overburden pressure and the hydraulic gradient can be increased. As the width of the suction area is small in the centrifuge, little air is trapped during percolation. Although the saturation degree is slightly smaller than that of the ground made by the former method, the ground by this method can be fully liquefied when subjected to shaking.

(2) Efficacy of model tests on liquefaction

Our team also revealed the efficacy of a centrifuge model test for liquefaction. Takahashi et al. (2006) showed the efficacy regarding the generation of excess pore water pressure in liquefied grounds surrounded by grid walls by using the modelling of models method. The modelling of models method is a technique to confirm that values converted to the prototype scale matches under several conditions in which the product of a centrifugal acceleration and model size ratio is unity. This is one of the methods to show the efficacy of a centrifuge model test. Figure 4.9 shows the relationship between the input acceleration and excess pore water pressure. It is found that experimental results overlapped even if a centrifugal acceleration and model size ratio are changed.

Fully liquefied ground easily flows depending on boundary conditions. The liquefied ground itself shows a fluid behaviour like a Bingham fluid. Takahashi et al. (2016) considered this fluid-like behaviour as that of fluid, and they showed the similarity rule. The liquefied ground has a relationship in which the shear strain rate and viscosity coefficient are roughly inversely proportional to each other, and the viscosity coefficient decreases corresponding to the model size ratio. Therefore, Reynolds's rule can be roughly satisfied along with Froude's.

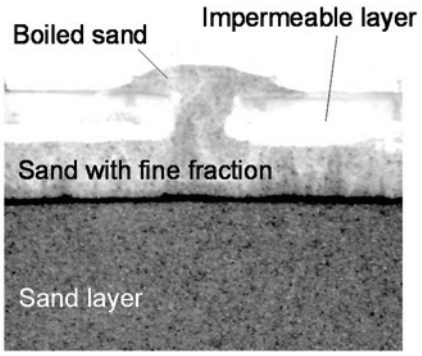

Figure 4.10 Sand boiling (based on Takano et al., 2016)

Viscous fluid is generally used as pore fluid to match the similarity ratios during times of dissipation of excess pore water pressure and dynamic behaviours. This method is called viscous scaling. Our team has also used this method many times. However, this method cannot satisfy the similitude ratio on viscosity, and it increases the viscosity; the ground is hard to flow when reproducing the lateral flow of liquefied ground and sand boiling from the liquefied ground. To solve this problem, our team proposed a method of mixing fine contents such as non-plastic silt with sand in order to decrease the permeability of the ground. This method does not use viscous fluid, and the viscosity of the liquefied ground can be maintained. For example, Takahashi et al. (2014) succeeded in reproducing a submarine landslide at which liquefied ground flew at high speed, and Takano et al. (2016) reproduced sand boiling due to liquefaction (see Figure 4.10).

4.3 Wave and current generator

(1) Centrifuge model tests of ocean waves

As mentioned above, it has recently become more important to understand ground behaviours subjected to waves in ocean and coastal areas. There are topics such as ocean development in the open sea, construction of wind turbines, natural disasters such as typhoons and tsunamis, submarine landslides, and sea level rise. Our team also expands the research scope for ground behaviours induced by the dynamic movement of fluids including high waves and tsunamis.

Sekiguchi & Phillips (1991) succeeded in reproducing ocean waves in a drum-type centrifuge, and Sekiguchi et al. (1995) did in a beam-type centrifuge in order to examine liquefaction due to wave cyclic loading.

Table 4.3 Types of wave generator

Type	Schematic view	Mechanism	Characteristic
Piston	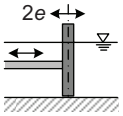	A vertical wave making plate reciprocates horizontally.	Suited for generating shallow water waves
Flap	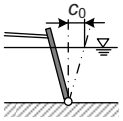	The top of a wave making plate reciprocates around the hinge at the bottom of a plate.	Suited for generating deep water waves
Quasi-flap	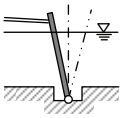	The hinge of the flap-type is embedded downward.	Higher efficiency of wave making than the flap-type
Plunger	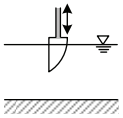	A triangular or curved plunger reciprocates vertically.	Suited for generating deep water waves
Pressure	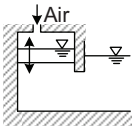	Air pressure in the chamber attached to a water channel fluctuates.	Suited for generating long period waves including tsunami

Thereafter, Baba et al. (2002) and Gao & Randolph (2005) also conducted wave tests in their drum-type centrifuges. They adopted either a plunger or flap-type wave generator. Table 4.3 shows the mechanisms and characteristics of representative wave generators. A plunger type is a generator in which a triangular or curved plunger reciprocates vertically and generates waves. A flap type is a generator in which the top of a wave making plate reciprocates around the hinge at the bottom of a plate. Both of them are suited for generating deep-water waves because they can move only water particles near the water surface. The advantage of these types of wave generator is that it does not need a large power, and it is appropriate for a centrifuge in which it is difficult to use large power. In addition, the wave generator in the past could produce only regular waves.

(2) Wave generators at early stage

Our team also designed a plunger-type wave generator in 2009 and investigated the stability of beach in a surf zone (Takahashi et al., 2010). It succeeded in producing waves, but the waveform was slightly unnatural. This would be because a plunger-type wave generator could fluctuate water only near the surface. This type of wave generator was considered to be unsuitable for producing waves in shallow water such as in a surf zone.

Next, our team developed a piston-type wave generator shown in Figure 4.11 (Takahashi et al., 2017). A wave making plate contacting a cam could be fluctuated

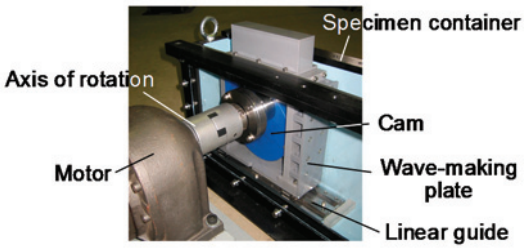

Figure 4.11 Wave generator at early stage (based on Takahashi et al., 2017)

in accordance with the rotation of the cam which was connected by a motor outside a specimen container. The wave making plate was positioned vertical to the bottom surface of the container and it fluctuated in the horizontal direction. As a result, it was possible to simultaneously move shallow- and deep-water particles, and this was suitable for reproducing waves in shallow water.

Takahashi et al. (2017) demonstrated the efficacy of waveforms, water pressure, and pore water pressure in a surf zone, using the modelling of models method. Figures 4.12 and 4.13 show wave breaking at 20*g* and 30*g* and time histories of pore water pressure in the model ground, respectively. It was confirmed that the behaviours at both centrifugal accelerations were quite similar. Takahashi et al. (2017) also showed the properties of the distributions of pore water pressure.

The stability of seawalls was also examined by our team (Takahashi & Morikawa, 2017). High waves induced by a typhoon frequently destroyed seawalls,

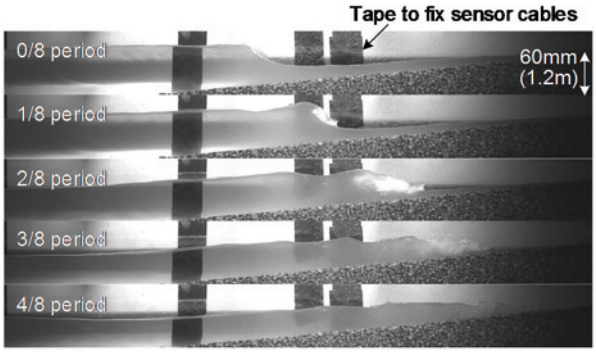

(a) Under 20*g*

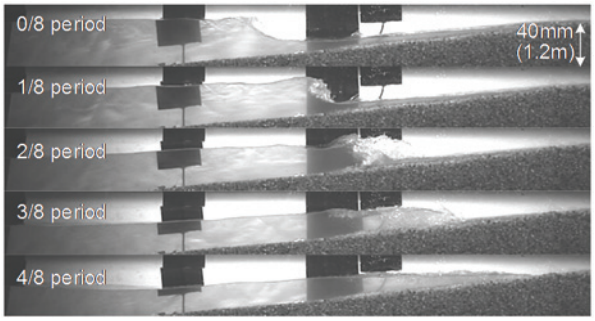

(b) Under 30*g*

Figure 4.12 Sequence pictures showing wave breaking (adapted from Takahashi et al., 2017)

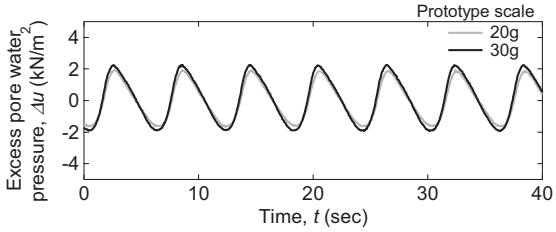

(a) G.L. -1.1m

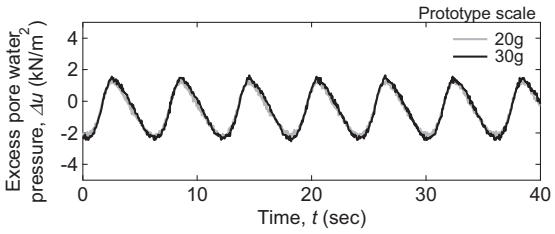

(b) G.L. -2.2m

Figure 4.13 Time histories of excess pore water pressure in ground (based on Takahashi et al., 2017)

containing ground failure. The mechanism of the failure was investigated by using a centrifuge. Figure 4.14 shows breaking seawalls with a sliding mode. This would occur because of the ground instability when the ground contained water and water in front of the seawall rushed back.

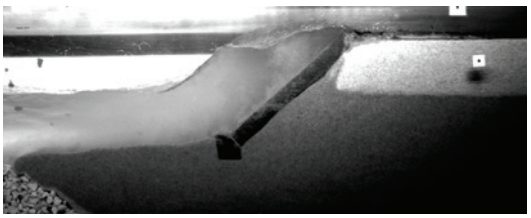

(a) Surge stage

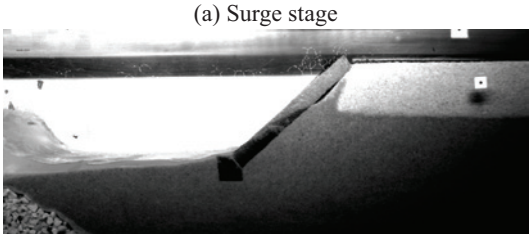

(b) Backwash stage

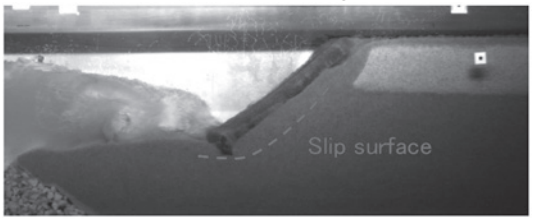

(c) Failure stage during backwash

Figure 4.14 Seawall failure during backwash (based on Takahashi & Morikawa, 2017)

(3) Development of wave and current generator

The wave generator mentioned above used a cam mechanism, and it could produce only regular waves. Whereas, in the real ocean, irregular waves with various time periods come to shores. As the difference in wave periods would affect the response properties of ground and coastal structures, it is important to understand the effect of wave periods by using irregular waves. In addition to the problem of waves, there was another problem that a water level in the model ground easily changed under the influence of the wave because the length of a specimen container was limited to approximately 1.5 m. To solve these problems, a new experimental device—named a wave and current generator—was developed. It can simultaneously generate current waves and flows, and it can adjust groundwater levels.

Figure 4.15 shows the schematic of the wave and current generator. A piston-type wave generator is installed in a specimen container, and it can be operated by a hydraulic cylinder. The displacement can be controlled with a hydraulic servo valve. Irregular waves can be generated by moving a wave making plate arbitrarily. A test run to generate irregular waves was conducted by using the model shown in Figure 4.16. To reduce reflected waves, a rubble mound was located on the corner of a specimen container. The expected significant wave height, $H_{1/3}$ and period, $T_{1/3}$ were 2.5 m and 12 s in a prototype scale, respectively. Figure 4.17

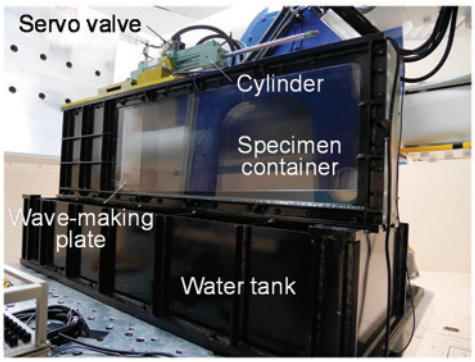

(a) Appearance

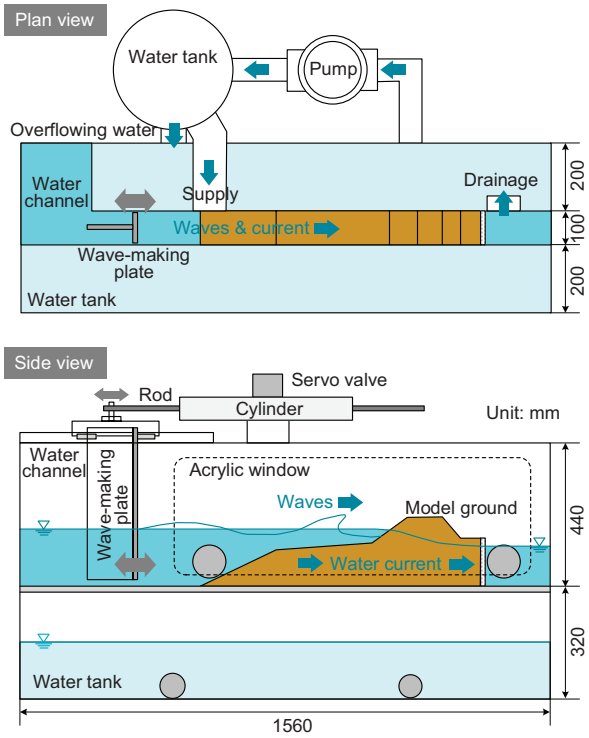

(b) Schematic drawing

Figure 4.15 Wave and current generator

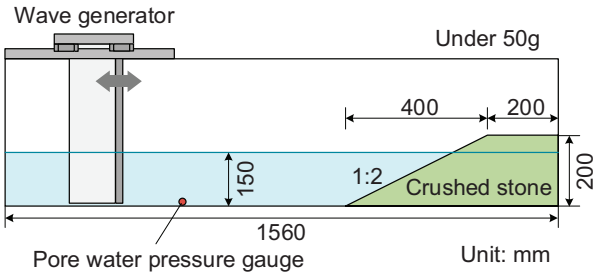

Figure 4.16 Schematic view of irregular wave tests using wave and current generator

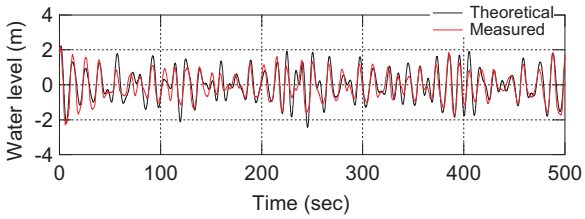

(a) Water level fluctuation

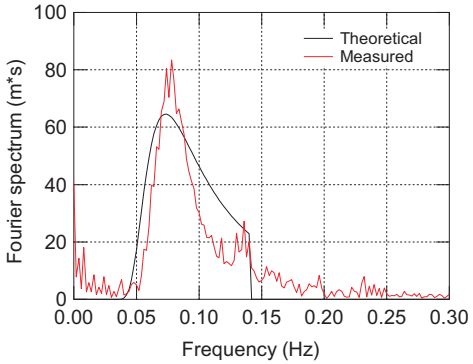

(b) Spectrum

Figure 4.17 Result of wave tests ($H_{1/3}$=2.5m, $T_{1/3}$=12s)

shows water-level fluctuation and its spectrum in a prototype scale. The water-level fluctuation was estimated by water pressure measured in front of the wave making plate, assuming the transfer function of 1.0 and the correction factor of 1.1. The figure also shows data estimated by the movement of a wave making plate. According to the potential velocity theory, a relationship between the half amplitude of a wave making plate and wave height is as follows.

$$F = \frac{H}{2e} = \frac{4\sinh^2\left(\frac{2\pi h}{L}\right)}{\frac{4\pi h}{L} + \sinh\frac{4\pi h}{L}} \qquad (1)$$

Here, h is the water depth and L is the wave length, which is the function of the wave period. The spectrum of the wave height can be theoretically estimated by the movement of a wave making plate and Eq. (1), and the wave height was gained by performing an inverse-Fourier transformation on the spectrum. The figure shows some disagreements between them. This would be due to reflected waves, the calculation of wave height from water pressure, and the estimation theory. However, the difference was not so large, and it can be said that the wave and current generator could almost produce proper irregular waves.

The wave and current generator carries tanks and a pump. These devices enable flow and keep water level differences in a specimen container. This test run succeeded in producing the inclined groundwater level in an embankment (see Figure 4.18). The groundwater level and pore water pressure in the ground affected the stability, and it is important to reproduce them.

4.4 Water supply tank

A large tsunami destroyed a considerable amount of infrastructure during the Great East-Japan Earthquake,

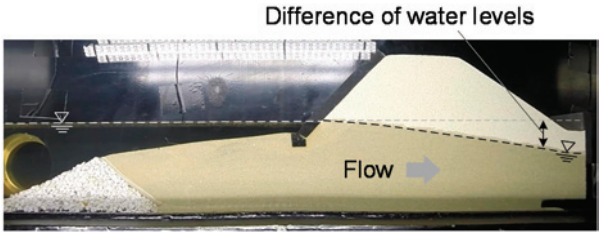

Figure 4.18 Slant water table in ground

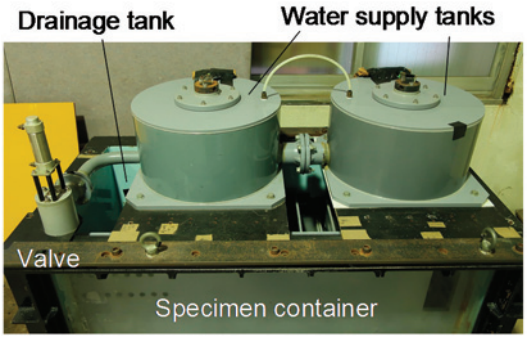

(a) Appearance

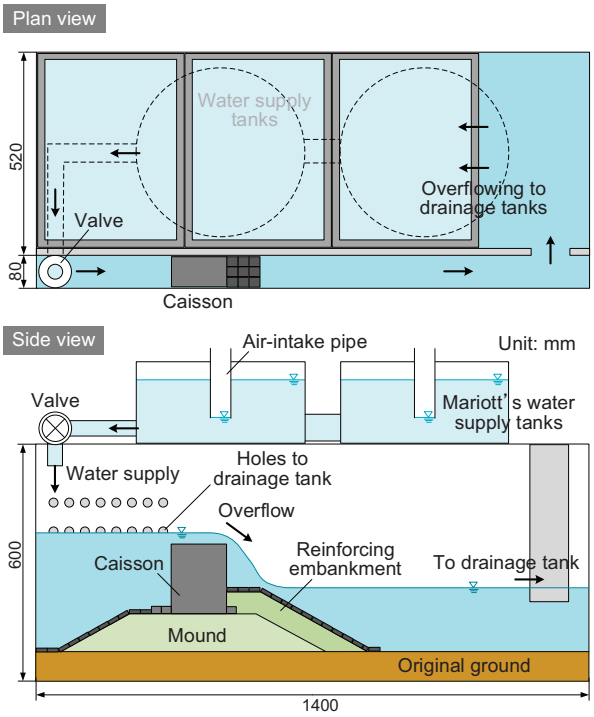

(b) Schematic drawing

Figure 4.19 Water supply tank

including breakwaters, levees, seawalls, and quay walls in coastal areas. Our research institute introduced a device for generating a tsunami in the centrifuge machine in 2013, for examining the failure mechanism, improving the design method for facilities, and designing countermeasures against tsunamis (Takahashi et al., 2015). To generate a tsunami, it is necessary to rapidly supply a large amount of water to one side of the model.

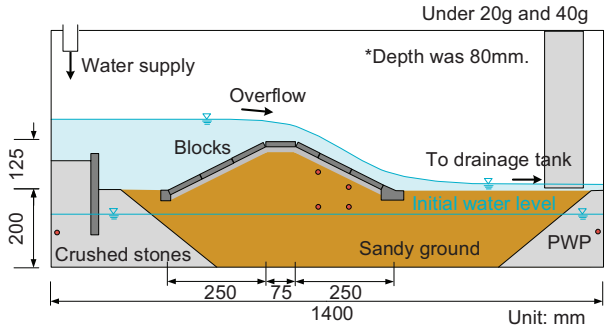

Figure 4.20 Schematic view of model for overflowing test against coastal levee (based on Takahashi et al., 2015)

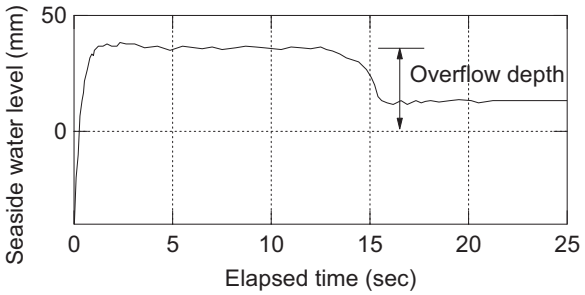

Figure 4.21 Water level in front of levee (based on Takahashi et al., 2015)

Recycling water is an ideal system in which drained water is pumped and re-supplied into the model. However, it was difficult to configure a pumping-up system because of the limitation of electric capacity. Therefore, a dam-break system supplying water once was adopted for the centrifuge.

Figure 4.19 shows the water supply tank manufactured; this equipment is detachable. The part where a structure such as an embankment is made is arranged on the side of the observation window, and a drainage tank is prepared behind it. A tank for supplied water is placed on the upper part of the specimen container. Under centrifugal acceleration, the valve is opened and water is supplied to the model. The amount of supplied water is constant because the tank installs Marriott's pipes. Supplied water flows in the model, and it is discharged to the drainage tank. The partition plate between the model and drainage tank has some holes so that water can flow into the tank. This flow can keep the water level at an arbitrary position.

Figures 4.20 and 4.21 show the schematic of an embankment model and time histories of water levels in front of the embankment (Takahashi et al., 2015). This test investigated the failure patterns of embankments under tsunami overflow. Figure 4.22 shows the situation in which a high water level in front of the embankment was kept and overflow occurred. Another example is a hydraulic test to examine the bearing capacity of breakwaters mounds under a tsunami (Takahashi et al.,

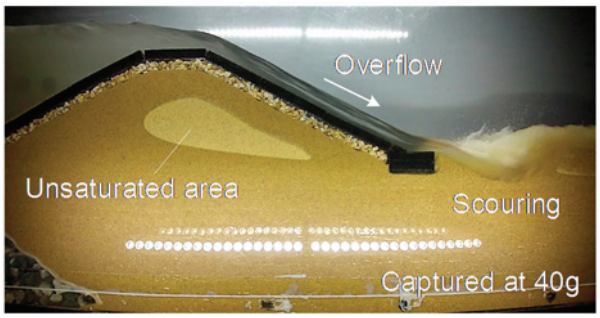

Figure 4.22 Appearance of overflowing (based on Takahashi et al., 2015)

2015). The bearing capacity was investigated, taking a seepage force inside the mounds into account. This result was adopted to the design method for breakwaters.

4.5 Image photographic devices

As it is impossible to quantitatively evaluate the kinematic behaviour of the model ground by direct observation of digital images, it is required to utilise an image analysis technology. Full field measurements using digital images has been adopted in the geotechnical engineering field, and it becomes possible to retrieve quantitative information from images; it is believed that this trend will continue. The movement was captured by a strobe camera installed outside the rotating body in the first and second machines. It was a mechanism to release the shutter at the moment the model came in front of the camera. Meanwhile, g-proof cameras on the platform are used for taking pictures now. The cameras used are categorised into two types: high-speed cameras and wearable cameras. The high-speed cameras are MEMRECAM GX-1 Plus and MEMRECAM Q1m manufactured by nac Image Technology Co., Ltd. These cameras can shoot images at a flame rate of 2,000 fps with 1,280 × 1,024 pixels in the centrifuge. A wearable camera is a Hero series made by GoPro, and several cameras are used for monitoring and recording the movement of a model.

The movement can be analysed by using photographed images with the particle tracking velocimetry (PTV) and particle image velocimetry (PIV) methods. There are many examples of image analysis by PTV, and an example in the early days is provided by Terashi & Kitazume (1988). Plastic bead targets were embedded into clay ground, and the movement of the beads were observed from an observation window. Recently, PIV, which is frequently used in experiments of hydrodynamics, has been used for centrifuge model tests (White et al., 2001). Our team also utilises this method (Takahashi et al., 2010). Furthermore, Takano et al. (2014) tries to read displacements from motion pictures and convert it to acceleration.

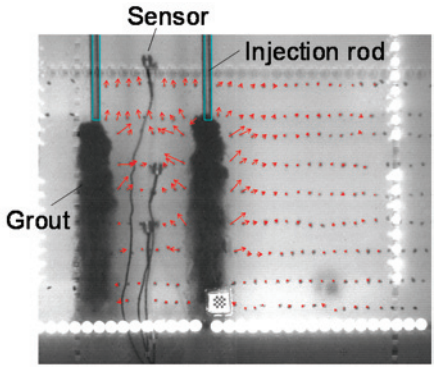

Figure 4.23 Ground displacement under static compaction (based on Takano et al., 2018)

Our team introduces a technique to visualise the movement of the ground using transparent granular soil, which can expose the movement inside the ground. This is a technique to make the model ground transparent by pouring fluids with a refractive index that matches that of quartz glass. The ground consists of pulverised quartz glass. Ezzein & Bathurst (2011) introduced this technology to the geotechnical engineering for the first time, and Takano et al. (2018) applied this to a centrifuge model test and adopted sugared water as fluid because it is easy to be used. Figure 4.23 shows grout squeezed into the transparent ground. The ground displacement could be examined by using this technique.

5. Summary

A centrifuge machine increases stress and water pressure in the model ground and produces the same behaviours of the prototype-scale structure. On the other hand, modelling prototype-scale structures and interpreting test results appropriately requires a certain skill set. Adequate management of a centrifuge model test will aid in comprehending the mechanism of ground behaviours. There are needs now to elucidate ground behaviours under a large earthquake, tsunami, and high tide and waves for ensuring the stability of civil engineering structures. Therefore, our research institute decided to introduce new systems and equipment which can reproduce large earthquakes and generate waves and flows in the centrifuge by renovating the second machine. The points of the renovation are as follows:

1) A large cowl and tail were attached to the main arms to reduce air resistance when operating the machine. This was needed because the capacity of a main motor was decreased. The attachment of a large cowl can also reduce wind hitting on a specimen container and equipment.

2) Both buckets were renewed, and the bucket for a tested model was enlarged and lightened. Additionally, the initial inclination angle was adjusted so that the direction of the resultant of the gravitational and centrifugal forces were nearly perpendicular to that of the platform surface at 50*g*.
3) A main motor and reduction gear box were updated as well. Two AC-type motors of 200 kW were used instead of a large DC-motor because this size of motor is cost effective. If a motor broke down in the future, the other motor could rotate the main arms although at a low speed and at a maximum acceleration of 30*g*. This will contribute to continuous research.
4) A shaking table and hydraulic power unit were updated to simulate large earthquakes. The maximum centrifugal acceleration and loading capacity were enhanced. Furthermore, the size of the top table was enlarged to allow using a large specimen container. A simple control system of using a servo valve and cylinder increases the stability of the system.
5) A wave and current generator was developed to reproduce waves and flows. This equipment has a piston-type wave generator operated by a hydraulic cylinder, and it can make irregular waves. In addition, it can generate flows and adjust groundwater levels.

In addition to these points, experimental technologies such as a measuring system, system for liquefaction model tests, water supply tank, and image analysis were developed and updated. We would like to perform valuable research by effectively utilizing these devices.

Acknowledgements

Nearly 40 years have already passed since the first centrifuge machine was developed in our research institute, but a centrifuge is still one of the main experimental facilities and remains a standard experimental tool in the geotechnical field. Furthermore, it has also been recently used for new applications such as reproducing waves and tsunami. Centrifuge modelling will be used for many experiments in the future.

Here, we would like to thank the Ministry of Land, Infrastructure, Transport, and Tourism and the people involved in the maintenance and renewal of the machine. Additionally, we thank Mr. Tetsuro Haraguchi, Mr. Daichi Munakata, Mr. Mitsuyoshi Torita, Mr. Ryoma Takeoka, and others from Nippon Steel & Sumikin Railway Technology Co., Ltd., who actively developed new technologies and manufactured the outstanding centrifuge machine.

Professor Masaki Kitazume of the Tokyo Institute of Technology, who belonged to our research institute in the past and was mainly involved in the development and maintenance of the second machine, gave us much advice on the renovation. When summarising this paper, we were informed about situations and problems during the development. Professor Hiroshi Katsuchi of Yokohama National University gave us advice on how to consider a drag force against cowls and carried out numerical analyses. As for the development of the new shaking table, we received considerable advice from Professor Gopal Madabhushi of Cambridge University, Dr. Sandra Escoffier of IFSTTAR, and Dr. Tetsuo Tobita of Kansai University. The Administrative, Coordination, and Disaster Prevention Department in our research institute have made efforts in administrative works. Mr. Takanobu Matsubara (Currently, a member of Shikoku Regional Development Bureau, Ministry of Land, Infrastructure, Transport, and Tourism) and Mr. Tomoki Uemura have shared renovation work as a group member. Without their cooperation, we could not perform this work. We would like to express our deep appreciation for them here.

Accepted Date: January 15, 2019

References

Avgherinos, P.J. and Schofield, A.N. (1969): Drawdown failure of centrifuged models, Proceedings of the 7th International Conference on Soil Mechanics and Foundation Engineering (ICSMFE), Vol. 2, pp. 497-505.

Baba, S., Miyake, M., Tsurugasaki, K., and Kim, H. (2002): Development of wave generation system in a drum centrifuge, Proceedings of International Conference on Physical modelling in Geotechnics (ICPMG), pp. 265-270.

Craig, W.H. (2002): The seven ages of centrifuge modelling, Proceedings of Workshop on Constitutive and Centrifuge Modelling: Two Extremes, Balkema, pp. 165-174.

Ezzein, F.M. and Bathurst, R.J. (2011): A transparent sand for geotechnical laboratory modeling, Geotechnical Testing Journal, Vol. 34, No. 6, pp. 590-601.

Gao, F.P. and Randolph, M.F. (2005): Progressive ocean wave modelling in drum centrifuge, Frontiers in Offshore Geotechnics (ISFOG 2005), Taylor & Fransis Group, pp. 583-588.

Inatomi, T., Kazama, M., Iai, S., Kitazume, M., and Terashi, M. (1988): Development of an earthquake simulator for the PHRI centrifuge, Proceedings of International Conference CENTRIFUGE 88, pp. 111-114.

Kazama, M, Inatomi, T., and Ohtsuka, K. (1988): Development of an earthquake simulator for the P.H.R.I. Centrifuge, Technical Note of the Port and Harbour Research Institute, No. 607, 35p. (in Japanese)

Kikuchi, Y., Kitazume, M., Suzuki, M., and Okada, T.

(2001): Structural property of double steel pipe sheet pile walls filled with premixed-soil, Technical Note of the Port and Harbour Research Institute, No. 997, 37p. (in Japanese)

Kitazume, M., Hayano, K., and Hashizume, H. (2003): Seismic stability of cement treated ground by titling and dynamic shaking table tests, Soils and Foundations, Vol. 43, No. 6, pp.125-140.

Kitazume, M. and Maruyama, K. (2006): External stability of group column type deep mixing improved ground under embankment loading, Soils and Foundations, Vol. 46, No. 3, pp.323-340.

Kitazume, M. and Maruyama, K. (2007): Internal stability of group column type deep mixing improved ground under embankment loading, Soils and Foundations, Vol. 47, No. 3, pp.437-455.

Kitazume, M. and Miyajima, S. (1995): Development of PHRI Mark II Geotechnical Centrifuge, Technical Note of the Port and Harbour Research Institute, No. 817, 33p.

Kitazume, M., Takahashi, H., and Takemura, S. (2003): Experimental and analytical studies on horizontal resistance of sand compaction pile improved ground, Report of the Port and Airport Research Institute, Vol. 42, No. 2, pp. 47-72. (in Japanese)

Kitazume, M. and Terashi, M. (1994): Operation of PHRI Geotechnical Centrifuge from 1980 to 1994, Technical Note of the Port and Harbour Research Institute, No. 787, 44p.

Mikasa, M., Takada, N., Yamada, K. (1969): Centrifugal model test of a rockfill dam, Proceedings of the 7th International Conference on Soil Mechanics and Foundation Engineering (ICSMFE), Vol. 2, pp. 325-339.

Morikawa, Y., Mizutani, T., Kikuchi, Y., Moriyasu, S., Taenaka, S., Takahashi, K., and Yokoyama, H. (2014): Performance evaluation of ground excavation and mixing by plural high pressure injection nozzles, Technical Note of the Port and Airport Research Institute, No. 1293, 28p. (in Japanese)

Nishimura, S., Takehana, K., Morikawa, Y., and Takahashi, H. (2011): Experimental study of stress changes due to compaction grouting, Soils and Foundations, Vol. 51, Issue 6, pp. 1037-1049.

Okamura, M. and Inoue, T. (2012): Preparation of fully saturated models for liquefaction study, International Journal of Physical Modelling in Geotechnics, Vol. 12, Issue 1, pp. 39-46.

Phillips, E. (1869a): De l'equilibre des solides elastiques semblables, Comptes Rendus de l' Académie des Sciences, Vol. 68, pp. 75-79. (in French)

Phillips, E. (1869b): Du movement des corps solides elastiques semblables, Comptes Rendus de l'Académie des Sciences, Vol. 69, pp. 911-912. (in French)

Sekiguchi, H., Kita, K., and Okamoto, O. (1995): Response of poro-elastoplastic beds to standing waves, Soils and Foundations, Vol. 35, Issue 3, pp. 31-42.

Sekiguchi, H. and Phillips, R. (1991): Generation of water waves in a drum centrifuge, Proceedings of International Conference CENTRIFUGE 91, pp. 343-350.

Takahashi, H. (2008): Fundamental study on the failure process of ground composed of sand piles and cohesive soil, Technical Note of the Port and Airport Research Institute, No. 1181, 155p. (in Japanese)

Takahashi, H., Kitazume, M., Ishibashi, S., and Yamawaki, S. (2006): Evaluating the saturation of model ground by P-wave velocity and modelling of models for a liquefaction study, International Journal of Physical Modelling in Geotechnics, Vol. 6, Issue 1, pp. 13-25.

Takahashi, H. and Morikawa, Y. (2017): Centrifuge model tests examining stability of seawalls subjected to high waves, Proceedings of the 19th International Conference on Soil Mechanics and Geotechnical Engineering (ICSMGE), pp. 971-974.

Takahashi, H., Morikawa, Y., Iba, H., Fukada, H., Maruyama, K., and Takehana, K. (2013): Experimental study on lattice-shaped cement treatment method for liquefaction countermeasure, Proceedings of the 18th International Conference on Soil Mechanics and Geotechnical Engineering (ICSMGE), pp. 1619-1622.

Takahashi, H., Morikawa, Y., and Ichikawa, E. (2010): Effects of rigid sidewall of specimen container on seismic behaviour, Proceedings of International Conference on Physical Modelling in Geotechnics (ICPMG), pp. 177-182.

Takahashi, H., Morikawa, Y., and Kashima, H. (2017): Centrifuge modelling of breaking waves and seashore ground, International Journal of Physical Modelling in Geotechnics, https://doi.org/10.1680/jphmg.17.00037.

Takahashi, H., Morikawa, Y., Mori, N., and Yasuda, T. (2015): Centrifugal model tests on collapse of coastal levee due to tsunami overflow, Geotechnics for Catastrophic Flooding Events, Taylor & Francis Group, pp. 353-358.

Takahashi, H., Ogawa, K., Hayano, K., Morikawa, Y., and Ninomiya, Y. (2010): Centrifuge model test on wave force resistance of artificial seashore reclaimed by granular treated soil, Annual Journal of Civil Engineering in the Ocean Vol. 26, pp. 687–692. (in Japanese)

Takahashi, H., Sassa, S., and Morikawa, Y. (2014): Centrifuge Modelling of earthquake-induced submarine landslide and its gravity flow transition,

Proceedings of International Conference on Physical Modelling in Geotechnics (ICPMG), pp. 1009-1015.
Takahashi, H., Sassa, S., Morikawa, Y., Takano, D., and Maruyama, K. (2014): Stability of caisson-type breakwater foundation under tsunami-induced seepage, Soils and Foundations, Vol. 54, Issue 4, pp. 789-805.
Takahashi, H., Sassa, S., Morikawa, Y., Watabe, Y., and Takano, D. (2015): Stability of caisson-type breakwater's mound and reinforcing embankment against tsunami, Report of the Port and Airport Research Institute, Vol. 54, No. 2, pp. 21-50. (in Japanese)
Takahashi, H., Takahashi, N., Morikawa, Y., Towhata, I., and Takano, D. (2016): Efficacy of pile-type improvement against lateral flow of liquefied ground, Geotechnique, Vol. 66, Issue 8, pp. 617-626.
Takano, D., Morikawa, Y., Miyata, Y., Nonoyama, H., and Bathurst, R.J. (2018): Physical modelling of compaction grouting injection using a transparent soil, Proceedings of International Conference on Physical Modelling in Geotechnics (ICPMG), pp. 1259-1263.
Takano, D., Morikawa, Y., and Takahashi, H. (2014): Full field measurement of liquefied soil on geotechnical centrifuge using digital image correlation, Proceedings of International Conference on Physical Modelling in Geotechnics (ICPMG), pp. 295-300.
Takano, D., Morikawa, Y., and Takahashi, H. (2016): Centrifuge modeling of sand boil on sand containing silt, Proceedings of the 15th Asian Regional Conference on Soil Mechanics and Geotechnical Engineering, pp. 875-879.
Takano, D., Nishimura, S., Morikawa, Y., and Takahashi, H. (2013): The effect of compaction grouting as a countermeasure against liquefaction, Report of the Port and Airport Research Institute, Vol. 52, No. 4, pp. 45-74. (in Japanese)
Terashi, M. (1985): Development of PHRI Geotechnical Centrifuge and its Application, Report of the Port and Harbour Research Institute, Vol. 24, No. 3, pp. 73-122.
Terashi, M. and Kitazume, M. (1988): Behavior of a fabric reinforced clay ground under an embankment, Proceedings of International Conference CENTRIFUGE 88, pp. 243-252.
Tomisaka, K., Iai, S., and Tobita, T. (2012): Detailed study of dynamic characteristics of the new geotechnical centrifuge at Disaster Prevention Research Institute, Kyoto University, Annuals of Disaster Prevention Research Institute, Kyoto University, No. 55B, pp. 201-214.
White, D.J., Take W.A, Bolton M.D., and Munachen S.E. (2001): A deformation measuring system for geotechnical testing based on digital imaging, close-range photogrammetry, and PIV image analysis. Proceedings of the 15th International Conference on Soil Mechanics and Geotechnical Engineering (ICSMGE), pp. 539-542.

港湾空港技術研究所資料　No.1353

２０１９．８

編集兼発行人　国立研究開発法人海上・港湾・航空技術研究所

発　行　所　港湾空港技術研究所
横須賀市長瀬３丁目１番１号
TEL. 046(844)5040　URL. http://www.pari.go.jp/

印　刷　所　株式会社シーケン